2013-05-06

An Improved Approach for Essential Tremor Spirography Processing by Integrating Frequency Domain Information and Spatial Domain Information

Keying Xu
University of Miami, canon8717@gmail.com

UNIVERSITY OF MIAMI

AN IMPROVED APPROACH FOR ESSENTIAL TREMOR SPIROGRAPHY PROCESSING BY INTEGRATING FREQUENCY DOMAIN INFORMATION AND SPATIAL DOMAIN INFORMATION

By

Keying Xu

A THESIS

Submitted to the Faculty
of the University of Miami
in partial fulfillment of the requirements for
the degree of Master of Science

Coral Gables, Florida

May 2013

UNIVERSITY OF MIAMI

A thesis submitted in partial fulfillment of
the requirements for the degree of
Master of Science

AN IMPROVED APPROACH FOR ESSENTIAL TREMOR SPIROGRAPHY PROCESSING BY INTEGRATING FREQUENCY DOMAIN INFORMATION AND SPATIAL DOMAIN INFORMATION

Keying Xu

Approved:

_____	_____
Weizhao Zhao, Ph.D.	M. Brian Blake, Ph.D.
Associate Professor of Biomedical Engineering	Dean of the Graduate School
_____	_____
Fatta Basil Nahab, M.D.	Jorge E. Bohorquez, Ph.D.
Assistant Professor of Neurology	Assistant Professor of Biomedical Engineering

XU, KEYING (M.S., Biomedical Engineering)

An Improved Approach for Essential Tremor Spirography Processing by Integrating Frequency Domain Information and Spatial Domain Information (May 2013)

Abstract of a thesis at the University of Miami.

Thesis supervised by Dr. Weizhao Zhao.
No. of pages in text (70).

Spirography is a standard neurological test that has been commonly used for essential tremor diagnosis and its severity assessment for years. Spirography requires simple hardware and software for data recording, which perfectly suits for clinical applications by its easy accessibility and useful and rich-information-contained outcomes that indicate tremor, tremor direction, tremor frequency, and other oscillation characteristics. However, current spirography analysis is handled by Fourier Transformation (FT) on acquired data only. Frequency spectrum information through FT, such as frequency distributions, magnitudes of selected frequencies, has been the only information reported in other studies. Further analysis on spirography is limited due to the loss and restraint of information during digitization, and the lack of valid processing procedures. This thesis provides a brief introduction of Essential Tremor and the application of spirography. In order to validate the algorithms developed in this study, we have created algorithmic simulations for smooth spirals and spirals with tremor oscillation. The developed simulation approach is the first of the two primary contributions of this thesis to the Essential Tremor study. Two chapters for spirography processing in frequency domain and spatial domain describe processing algorithms applied to simulated data sets and

tremor patients' spirography data sets. These two chapters discuss, test and compare two methods in frequency domain analysis to get the dominant frequency related information, along with two methods in spatial domain analysis, one aiming at unwrap the spiral-wired graph, the other designed to quantify the amplitude of tremor oscillation movement. The developed method in spatial domain is the second of the two primary contributions of this thesis to the Essential Tremor study. In the Discussion and Conclusion Chapter, we discuss current obstacles in spirography analysis and further development direction. Suggestions to handle patient spirography data are also provided in this Chapter.

TABLE OF CONTENTS

LIST OF FIGURES

LIST OF TABLES

LIST OF ABBREVIATIONS

DF	Dominant Frequency/ Predominant Frequency
DFA	Dominant Frequency Amplitude
ET	Essential Tremor
FD	Frequency Domain
FFT	Fast Fourier Transformation
SD	Spatial Domain

Chapter I: Introduction

1. Essential Tremor

1.1 What is Essential Tremor

Essential tremor (ET) is the most common cause of pathological tremor and one of the most common neurological diseases [1–3]. Its diagnose is based on clinical grounds, misdiagnosis occurs in up to 50% of cases. Parkinson's disease (particularly in elderly patients) and dystonia (tremulous cervical dystonia) are the most common disorders mistaken for ET [1,2].

Essential Tremor was defined by the Movement Disorder Society Consensus Statement on Tremor (1998) as "a bilateral, largely symmetric postural or kinetic tremor involving hands and forearms that is visible and persistent". To diagnose Essential Tremor, other causes for tremor must be excluded (dystonia, psychogenic tremor, task-specific tremor, tremorgenic drugs, primary orthostatic tremor, position-specific tremor, isolated voice tremor, isolated tongue or chin tremor, and isolated leg tremor). The neurological examination must be normal, with exception of the cogwheel phenomenon meanwhile symptom duration needs to be longer than 3 or 5 years (Froment's sign) [5].

The frequency of the kinetic tremor typically ranges form 8Hz to 12Hz, and is related to age inversely [1–3,5,6]. Tremor may occur also in the legs, feet, trunk, jaw (chin), tongue, and voice [1–3,5–8]. In general ET affects the upper limbs in most cases (95% of patients), and according to Deuschl and Elble, less commonly affects the head (30%), voice (20%), jaw (10%), tongue (20%), trunk (5%) and lower limbs (10%) [8].

The prevalence of ET is estimated to be 4.0%–5.6% among individuals aging >40 years [9,10] and 9.0% or higher among individuals >60 years of age. The etiologies of this widespread disease are likely to be diverse. Indeed, both genetic [11–14] and environmental [15–19] factors are implicated.

1.2 Essential Tremor Pathology

It has been implicated that the cerebellum might be involved in ET centrally. First, cerebellar-like problems, with abnormalities in tandem gait and balance, have been described in ET patients repeatedly [20–24]. Intention tremor of the hands occurs in 58% of ET patients [25,26], and, spreads to the head in 10% of ET patients [27]. Second, unilateral cerebellar stroke has been reported to abruptly terminate ipsilateral arm tremor in ET [28] while cerebellar outflow pathways are targeted in deep brain stimulation, which is an effective treatment for ET [29,30]. In addition, numerous neuro-imaging studies have provided evidence of cerebellar hemispheric dysfunction in ET, including positron emission tomography [32–39], functional magnetic resonance imaging (fMRI) [31], and [1H] magnetic resonance spectro- scopic imaging (MRSI) studies [40,41].
As in genetic study, only a few genes/loci have been nominated, which together explain a fraction of ET heritability. Further understanding of the genetic background of ET is hoped to help design future therapeutic strategies targeting the molecular events that cause neuronal loss/dysfunction [42].

1.3 Essential Tremor Types

According to a paper published in 2012, *Essential Tremor: phenotypes*, ET types have been categorized in several different ways through time:

> *In 1981, Marsden et al. classified ET in four different types: type I: exaggerated physiological tremor; type II: benign pathological ET (with good response to alcohol use and propranolol and familial history), type III: severe pathological ET (with no familial history and no response to alcohol use or propranolol), and type IV: symptomatic ET (associated to other neurological condition, such as dystonia and peripheral neuropathy) [4].*
>
> *In 1987, Deuschl et al. classified ET in two types: Type A, with preponderant synchronous activity in antagonists under postural conditions; type B, with preponderant alternating activity in antagonists [4].*
>
> *In 2009, Deuschl and Elble proposed a subclassification of ET into three categories: hereditary ET (patients fulfill the consensus criteria for definite or classic ET, with unequivocal family history and the onset or tremor occurring before age 65), sporadic ET (patients fulfill the consensus criteria for definite or classic ET, with age of onset before age 65, but without family history of tremor), and senile ET (patients fulfill the criteria for definite or classical ET, with or without family history of tremor, but develop tremor after age 65) [8].*
>
> *Recently, the concept of ET has evolved into two different pathways. First of all, the classical ET, as a monosymptomatic disorder (due a dynamic oscillatory disturbance of the motor system), and second, a heterogenous disorder, the Essential Tremors, or a family of diseases (a more complex and heterogeneous degenerative disorder) [2,8].*
>
> *Louis et al. described clinical subtypes of ET, with differences in age of onset (a bimodal distribution: second–third decades versus sixth and seventh decades), anatomic distribution of tremor (isolated head tremor 3.3%, head and arm tremor 13.3%, and arm tremor without head tremor 83.3%), and rate of progression (slow or rapid progression) [43].*

ET phenomenology is classified in both motor and non-motor elements in current concepts.

1.4 ET with Motor Features:

A paper published in 2012 pointed out that although the most recognizable and defined feature in patients with ET is a kinetic tremor of the arms, the older view that this is a monosymptomatic disease is no longer tenable [44]. First, the tremor phenomenology itself is diverse and multifaceted. In addition to kinetic and postural tremor, intention tremor [25], and tremor at rest [45–47] may occur. Furthermore, the relative severity of different tremor types (kinetic > postural rather than the converse [48]), the favored sites of anatomical involvement (arm > head > jaw [49,50]), and the typical direction of somatotopic spread (from arms to head rather than the converse) [51] are distinctive. Second, aside from the tremor phenomenology, other motor features have been described in ET. Perhaps most important of these are the complaints of gait difficulty, which are not uncommon in patients with ET.

The main phenotypes of ET with motor features collated by Heʹlio A.G. Teive:

> *1. Classical ET with hand tremor: Typically a bilateral, symmetric postural or kinetic tremor, with flexion–extension movement of the hand/arms and an adduction–abduction movement of the fingers [1,2,4,8].*
>
> *2. ET with head tremor: In general head tremor is associated with mild arm tremor and isolated head tremor is very rare (with presentation of hand tremor before the appearance of head tremor). Commonly the head movements occur in a vertical or horizontal plane and Charcot defined it as yes/yes and no/no tremor. Postural tremor may occur in the head in 34% to 53% of patients with ET [1,2,4,8]. In 2006, Leegwater et al. described intentional tremor of the head in patients with ET [52]. Louis and Dogu, in a population-based and clinic-based case sample, stated that head tremor in the complete absence of arm tremor was not observed in any cases (0.0%) [53]. Quinn et al. stated that an isolated head tremor is frequently associated with spasmodic torticollis [2].*
>
> *3. ET with jaw tremor: Louis et al. observed that jaw tremor was present in 28.6% of ET cases with consistent rest tremor and in 7.8% of cases without rest tremor. ET cases with jaw tremor had a more clinically severe and more*

> *topographically widespread disorder. The main differential diagnosis is made with Parkinson's disease and dystonia [54].*
>
> *4. ET with tongue and voice tremor: Frequently tremor in these regions occurs in association with hand tremor. Many patients with isolated voice tremor have laryngeal dystonia [1,2,4,8].*
>
> *5. ET with trunk and leg and feet tremor: This is a infrequent form of ET, and Poston et al., in a series of 63 ET cases, found kinetic leg tremor in only 14.3% [1,2,4,8].*

Other motor features described in patients with ET are gait ataxia, postural instability and eye-motion abnormalities [1,2,8]. There are clinical and electrophysiologic evidences of a pancerebellar disturbance in patients with ET.

1.5 ET with Non-Motor Features:

While traditionally defined as a motor disorder without cognitive features, work over the past 20–30 years has shown that non-motor features, both psychiatric and cognitive, are a feature of that ET as well [55–58].

The non-motor features of ET may be divided into cognitive and psychiatric. Cognitive features, especially problems with executive function, were first appreciated in a 2001 study of Gasparini et al. [59] and then by other investigators in that same year [60] and soon after [61–65].

Cognitive abnormalities are not just a feature of a small self-selected group of severe ET cases attending a surgical center or a specialty clinic, but a broader and more elemental disease-associated phenomenon. Summarized by Tröster et al. [63] in various studies, ET patients have demonstrated significantly lower than expected scores on measures of visual attention, complex auditory, verbal fluency, and immediate recall. These types of deficits could reflect difficulty with initiation and maintenance of information processing

strategies. This mechanism is similarly thought to underlie cognitive changes in patients with Parkinson's disease. In the population-based study of Benito- Leon et al. [64], forgetfulness was reported in 43.1% of controls and 50.4% of ET patients, a marginally significant difference ($p = 0.05$), and which raised the possibility that the cognitive deficits in ET may not be entirely subclinical and may indeed be noticeable to patients.

A population-based study in 2006 in Madrid conducted by Benito-Leon et al. [66] was the first to demonstrate that the odds of dementia were nearly twice as high among older onset ET cases than age-matched controls without tremor. More recently, in a second population-based study of the elderly in northern Manhattan, statistics shows that ET was associated with a near-doubling of the odds of prevalent dementia [67], therefore confirming the results of the initial study in Madrid. The study in Spain reported that 83.9% of the demented ET cases reported tremor preceded the onset of dementia rather than the converse [66], which suggests that ET led to dementia.

Other than cognitive features of ET, a number of psychiatric correlates have come into notice in recent years. In one of these studies [68], patients with ET were characterized as scoring higher in harm-avoidance performances, which means that they were more worrying and shy than controls. The scores didn’t correlate with the tremor severity or with objective and subjective scales of disability. It is possible that the personality profile observed was not entirely related to functional disability caused by tremor. In other words, it may have been a primary disease feature [68].

Studies also show that anxiety [69], depressive symptoms [70–73], and social phobia [74] have also been expressed in ET patients to a greater extent than in controls [75,76]. Considering that depression may be a consequence of the tremor and disability, it is

possible that a mood disorder is part of the underlying disease process rather than a response to the tremor.

2. Spirography Studies

Spirograph is the recording of the drawing of an Archimedean spiral, in this study following the trace of a standard model spiral on the plan of drawing, with or without involuntary element.

All information of each drawing recordings are saved in a text file with .spr as file extension. Each recording file includes in the first several lines information of patient name, gender, age, date of recording and a brief description concerning individual conditions. All those information are optional at the time of recording therefore availability of those information depends on whether the operator has put it in since the recording or not.

Spiral drawing information is recorded as location coordinates obtained at certain sampling frequency in chronological sequence. In other words, the tablet records the location of the pen point in the designated region as pairs of rectangular coordinates in the order of time with certain fixed time interval. This sampling frequency is decided by tablet hardware and recording software, the product of the index number of each coordinate pair and sampling frequency is the time stamp of this point relative to the starting of the recording. As the result of the time stamp, other than traditional spirography test in which patient draw on a piece of paper that records a final image with spatial information only, time domain information is preserved therefore makes reproducing the process of drawing possible.

Recording data displays as figures below,

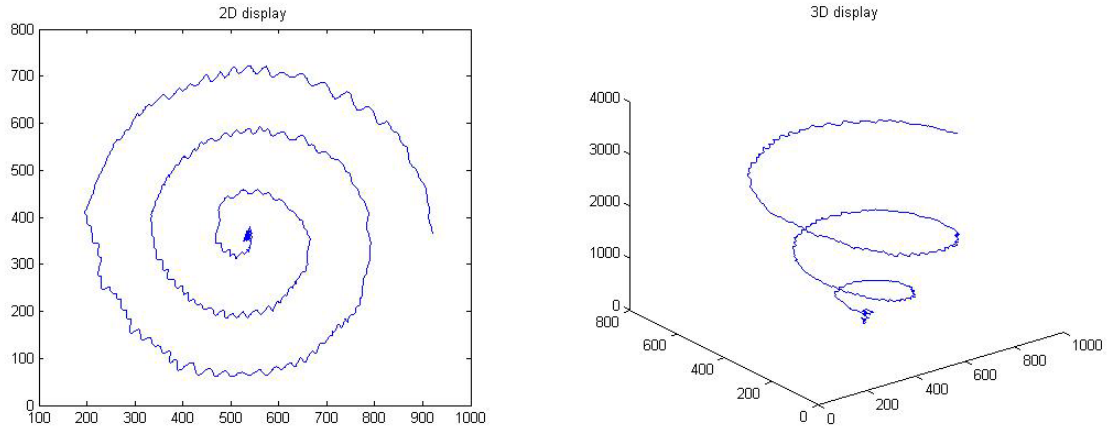

Figure I.3.1, Patient recording raw data. Left: 2D final drawing image; right: 3D display with z-axis as time.

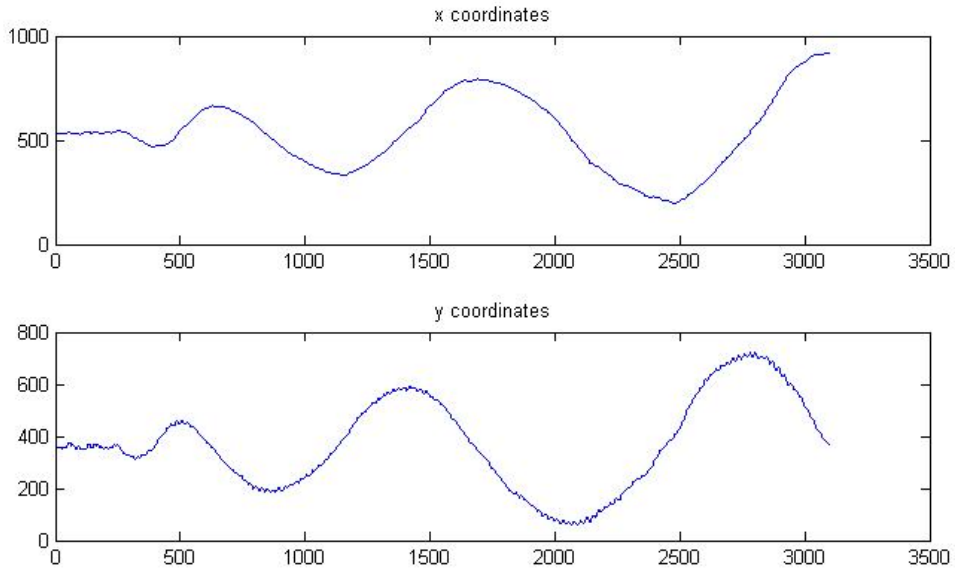

Figure I.3.2, Patient recording raw data. Upper: x coordinates of each point (pen point projection on x-axis) in the order of time; lower: y coordinates of each point (pen point projection on y-axis) in the order of time.

Because all spatial information are time stamped as shown in the figures above, time domain indicators such as velocity and acceleration at each point/time as well as

frequency domain features become available. Details of frequency domain analysis are elaborated in Chapter III.

3. Problem Statement and Significance

Spirography has been a commonly used test in tremor diagnosis. However there is no standard post processing method, resulting in individual standalone studies but no cross research data analysis. This is mainly because of the lack of a standard recording procedure and compatible device. In the recording of spirographies, different recording devices and recording principle would lead to differences in data source, data type, data format and data organization. Meanwhile different subject instructions during recording such as whether a time limit is given for each drawing also bring about dynamics into the recordings. Post recording process procedure is highly depended on the recorded data (including type, format, organization, information indicated) and the intended parameters for spirography analysis. In spite of the differences among each study, almost all studies are interested in the frequency of tremor oscillation and dominant frequency reading in frequency spectrum or power spectrum.

In this study, spatial domain analysis and frequency domain analysis processing procedures are developed based on prerecorded databases. Simulations are conducted during algorithm development and reliability tests.

4. Study of Interest

In describing a movement in space, the representative parameters are velocity and direction. In describing an oscillation, the representative characteristics are frequency and

amplitude. In this study, velocity is an intermediate parameter and input data for the processing procedures that follows. The demanded parameters of interest are oscillation direction, tremor frequency and oscillation amplitude.

4.1 Tremor Velocity:

Velocity is excluded from the final output for the following reasons.

- As a result of the nature of oscillation movement, average velocity of the process is representable and therefore replaceable with oscillation frequency and oscillation amplitude (4 times amplitude times frequency equals distance traveled in one second), yet this representation transformation is not reversible.
- Real time velocity mapping is simply a first order transform result of location data, it has as many elements as the number of coordinates pairs in the recording data, which means the same size of recording in processing and storage yet no further information.
- Real time velocity data is repetitive (the nature of oscillation movement) and redundant data rather than extracted refined information.
- Tremor velocity differs from patient to patient, it is highly differentiated because of individual differences and therapeutic conditions.

However, in this study, tremor velocity is used for frequency analysis. Because tremor oscillation axes usually does not align perfectly with coordinate axis, which means movement trace on neither axis may represent the frequency information fully, but partial spatial information only. Velocity defined as the distance travelled per unit time would neglect the direction of movement, which is not of interest in frequency analysis, while

preserves all amplitude information. The importance of amplitude analysis will be demonstrated in later chapters.

The following figure displays the velocity spectrum and acceleration spectrum of a patient recording.

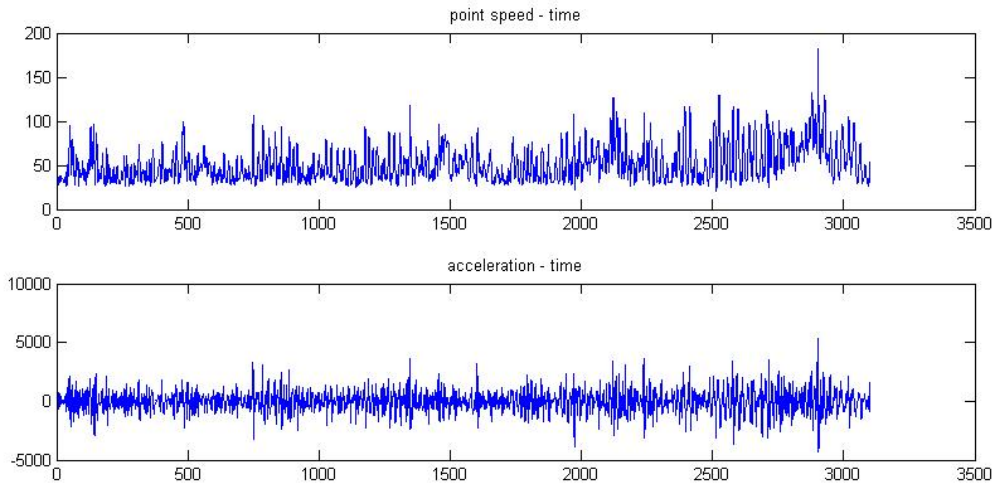

Figure I.4.1 Time domain spectrum of a tremor patient recording. In the upper frame is Velocity vs. tp, in the lower frame is the corresponding acceleration spectrum.

4.2 Tremor Direction:

Because the direct cause of tremor is the miscorrelation of the contractions of antagonist muscle, the backward and forward bidirectional movement has an existing oscillation axis that is mostly steady and consistent with the posture of limb. The problem with documenting these directions for further matching and statistical analysis is that the direction recorded is highly related to the position of the limb to the recording device, which is unlikely to be delicately manipulated to share a same registration with others precisely when it concerns with different recordings from the same patient. In the case of

recordings from different patients, similar to the dilemma of velocity, tremor direction is highly differentiated without apparent pattern.

However, in this study, direction information is taken into account and applied as an intermediate parameter for tremor amplitude (oscillation amplitude) analysis.

The following figure displays the difference of tremor directions between two recordings caused by position shifting, which is inevitable.

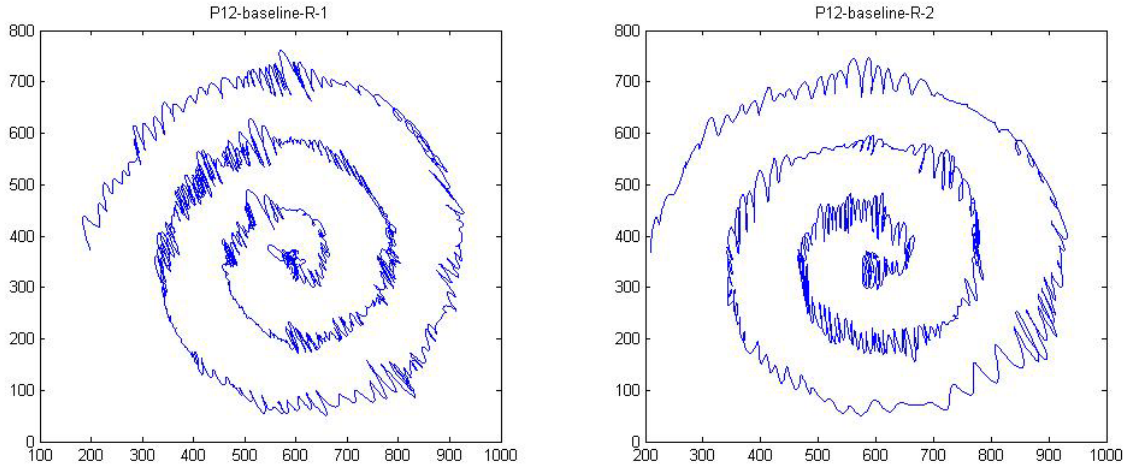

Figure I.4.2 Tremor direction. On the left is the final image of tremor patient recording, on the right is the final image of another recording of the same patient under the same condition (baseline, no alcohol, no medication), the second recording was conducted within 2 minutes after the first one. The slight tremor direction change is caused by difference of arm placement, an uncontrollable position change.

4.3 Tremor Frequency:

Frequency is one of the basic characteristics of oscillation movement. According to observation, the pace (frequency) of involuntary oscillation movement of essential tremor patient does not undergo abrupt changes, which means there is a consistent predominant tremor frequency, it is either a sharp spike in the frequency spectrum or is a bump with a center and certain bandwidth. It is also a common observation that although predominant

frequency differ from patient to patient, it remains considerably consistent for individual patient within any short-term unless under influence like alcohol or medications.

Although the pathology behind Essential Tremor is not clear, it is well recognized that the mechanism of any muscle activities, whether voluntary or involuntary, starts with series of nerve signals from motor cortex. These series of signals travel all the way down to neuromuscular junction (nerve-muscle interface) and stimulate muscle fibers, which result in muscle contractions hence body movement. Consistent involuntary body movement frequency displayed in tremor patients indicate consistent firing rate of stimulations (disturbance) whether comes from the cortex or integrated in or misaligned during downstream. For those reasons discussed above, frequency spectrum especially predominant frequency is an important symptom indicator in tremor severity assessment and long-term pathography analysis.

The following is a figure showing frequency spectrum of velocity and acceleration of a patient recording.

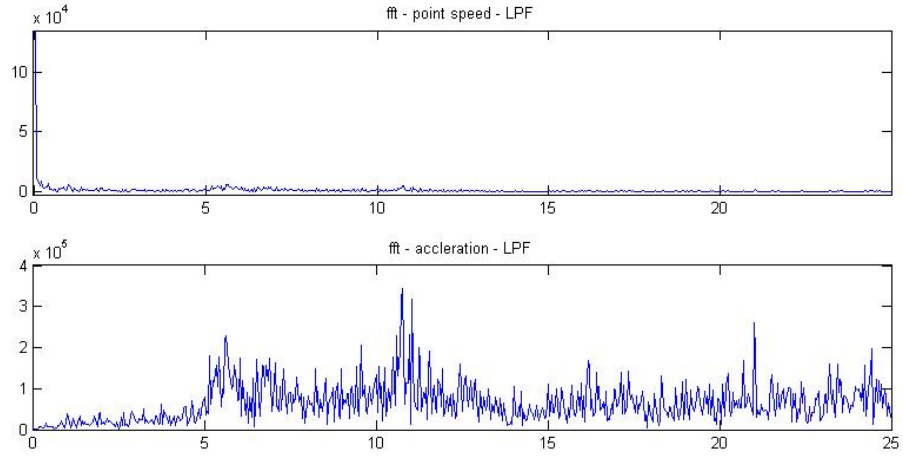

Figure I.4.3Frequency spectrum of a patient recording. Predominant frequency is around 11 Hz. Dominant frequency of tremor oscillation is around 5.5 Hz due to frequency doubling, which is elaborated with the principle and method of peak choosing in Chapter III.

4.4 Tremor Amplitude:

Like frequency, amplitude is also a common characteristic of oscillation movement. Tremor movement is bidirectional, if break down into the smallest repetitive unit, it is a series of acceleration in one direction, deceleration in the same direction, acceleration in the opposite direction, deceleration, acceleration in the original direction. Like the way distance is influenced in a simple acceleration-deceleration process, tremor amplitude depends on the duration of each oscillation (frequency's reciprocal) and the force of acceleration, the latter of which varies because of muscle capacity (fatigue, age) and medication status for each individual patient. However the factors of amplitude either would not undergo dramatic change in short-term (muscle capacity) or is controllable (medication and other conducted influences). Though it is not used as a precise indicator for assessment, amplitude is a worthwhile parameter.

5. Software Used to Record and Process Spirography

The software used in patient recording device is Python. Python is a general-purpose programming language that features code readability. Python's syntax allows programmers to express concepts by straightforward coding and constructs clear programs in either a small or large scale. Python is often used as a scripting language, but is also used in a wide range of non-scripting contexts. Using third-party tools, Python codes can be built into standalone executable programs.

The programming platform used in post-recording processing is MATLAB. MATLAB (matrix laboratory) is a fourth-generation programming language and interactive environment for numerical computing, visualization, and programming. Developed by

MathWorks, MATLAB allows matrix manipulations, plotting of functions and data, implementation of algorithms, creation of user interfaces, and interfacing with programs written in other languages, including C, C++, Java, and Fortran.

6. Predetermined Parameter Acquisition

As mentioned before, the series of spirography analysis is conducted with digitized data, as a result, certain predetermined parameters are to be tested and unified so that results could be transformed into universal units comparable to other researches throughout the entire processing.

Those parameters are:

Sampling Frequency in recording is 125Hz. 6 test recordings were taken for this calibration. A cellphone stopwatch was used for the timing of each recording.

Spatial Resolution of tablet is 4 pixels/mm or 0.25mm/pixel. 17 test recordings were taken for this calibration. A stationary ruler was used to draw a 10 cm line for each test, maximum and minimum value were excluded before averaging, the nearest integer of mean value was assigned as test result.)

Standard Spiral

Right hand model spiral:

$$\begin{cases} X(t) = 585 - \dfrac{380 \times t}{tp} \times \cos(\dfrac{6\pi \times t}{tp}), & t = 1 \ldots tp \\ Y(t) = 350 - \dfrac{380 \times t}{tp} \times \sin(\dfrac{6\pi \times t}{tp}), & t = 1 \ldots tp \end{cases} \tag{1.1}$$

Left hand model spiral:

$$\begin{cases} X(t) = 535 + \dfrac{380 \times t}{tp} \times \cos(\dfrac{6\pi \times t}{tp}), & t = 1 \ldots tp \\ Y(t) = 350 - \dfrac{380 \times t}{tp} \times \sin(\dfrac{6\pi \times t}{tp}), & t = 1 \ldots tp \end{cases} \tag{1.2}$$

Where *t* is the sampling time, *tp* is the number of sampling points, all units are in pixel.

In this report, only right hand recordings were used for analysis demonstration. The recording system and the analysis procedure are designed for recordings from both hands. More than 6 test recordings each were taken for this calibration to find the center, ending point and radius parameter of the standard spiral under left hand recording mode and right hand recording mode respectively.

Chapter II: Data Sets Used During Research

1. Algorithmic Simulation

In order to test and verify the spirography data collected from clinics, we first generated sequences of simulated spirographies. Algorithmic simulation is used to obtain regulated characteristics embedded in data for validation test. The designated outcomes of simulation are data series in the same format as the raw data read from real patient recording, containing user-defined/assigned information. In another word, simulation is to manufacture data series with known information. Two categories of simulations have been constructed in the thesis research: spiral simulation and tremor simulation.

1.1 Spiral Simulation:

An Archimedean spiral in a 2-dimentional rectangular coordinate system can be defined as parametric curve:

$$\begin{cases} x = xc + \frac{u}{r}\cos u & u = 0...k\pi \\ y = yc + \frac{u}{r}\sin u & u = 0...k\pi \end{cases} \tag{2.1}$$

Where (*xc, yc*) is the coordinates of the center (starting point) of the spiral; *u/r* is the radius increment of every 2π radian (every one full circle, the larger the value *r*, the smaller the increment); $k\pi$ is the radian covered by the spiral from the starting point to the ending point; *u* is an array with components start from *0* to $k\pi$ (each element of *u* corresponding to one point on the spiral). The smaller increment of *u*, the higher spatial resolution (smoothness) of the spiral; the larger *k* value, the longer the spiral.

If *1/r* is substitude by *d,* The formula could also be writen as follow:

$$\begin{aligned} x &= xc + u \times d \times \cos u, & u &= 0 \ldots k\pi \\ y &= yc + u \times d \times \sin u, & u &= 0 \ldots k\pi \end{aligned} \tag{2.2}$$

Now that it is known that the data saved in the recording files are location coordinates in chronological sequence at certain sampling frequency (125Hz in this study), the values of *xc, yc, d* and *k* are predetermined by the modal spiral selected. The number of elemnets in *u* is determined by the duration of the simulated recording (element count *tp* = recording duration × sampling frequency 125Hz). The only variable is the element *u* which corrspond with the time domain information (pace) of the spiral drawing. *(x(n),y(n))* stands for the coordinate pair of the *n*'s point, they are the *x* and *y* coordinate in the simulated drawing. The order of those *(x(n),y(n))* pairs is the order of the corresponding points drew with n-time interval (0.008sec = 1/125 Hz). Therefore the *u* element increment (*u(n)~u(n +1)*) has a first-order relationship with the velocity of spiral drawing. There are two paces of spiral drawing in general: drawing with constant angular velocity (the same radians passed during any unit interval, rad/sec or degree/sec) or drawing with constant linear velocity (travel the same distance at any unit interval, pixel/sec or mm/sec).

a. Constant angular velocity: Spiral1

In this mode, the radian covered at each interval is a constant. Value of *u* undergoes arithmetic progression. Δ*u* is the increment of *u* element.

$$\begin{aligned} \Delta u &= \frac{k\pi}{tp} \\ u(n+1) &= u(n) + \Delta u, \quad u(1) = 0 \qquad n = 1 \ldots tp \end{aligned} \tag{2.3}$$

This could also be written as

$$u(n) = \Delta u \times (n-1), \qquad n = 1 \ldots tp \tag{2.4}$$

Therefore the formula of Archimedean spiral can be written as

$$\begin{aligned} x(n) &= xc + \Delta u \times (n-1) \times d \times \cos(\Delta u \times (n-1)), && n = 1 \ldots tp \\ y(n) &= yc + \Delta u \times (n-1) \times d \times \sin(\Delta u \times (n-1)), && n = 1 \ldots tp \end{aligned} \tag{2.5}$$

Since Δu is a constant that represents the gradient of radians and $\Delta u \times d$ is a constant that represents the gradient of radius, substituting with amplitude/radius coefficient *amp,* the above equations can be written as:

$$\begin{aligned} x(n) &= xc + amp \times (n-1) \times \cos(\Delta u \times (n-1)), && n = 1 \ldots tp \\ y(n) &= yc + amp \times (n-1) \times \sin(\Delta u \times (n-1)), && n = 1 \ldots tp \end{aligned} \tag{2.6}$$

Above equations are equivalent to their one sampling point shift

$$\begin{aligned} x(n) &= xc + amp \times n \times \cos(\Delta u \times n), && n = 1 \ldots tp \\ y(n) &= yc + amp \times n \times \sin(\Delta u \times n), && n = 1 \ldots tp \end{aligned} \tag{2.7}$$

Where $radian(n) = \Delta u \times n$. Considering the direction of the spiral extension, value *amp* is negative for clockwise spiral and positive for counterclockwise spiral.

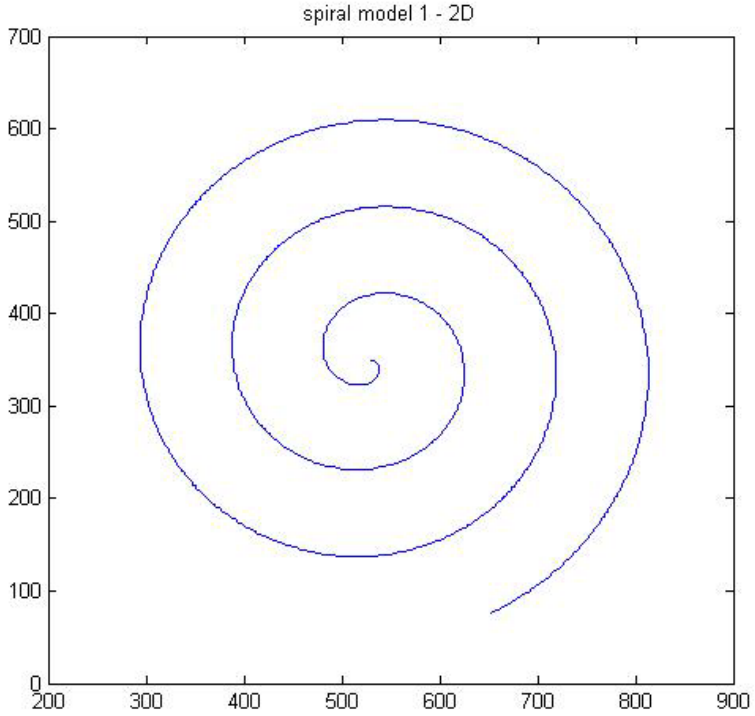

Figure II.1.1 Spiral1 generation mode, 2D final image.

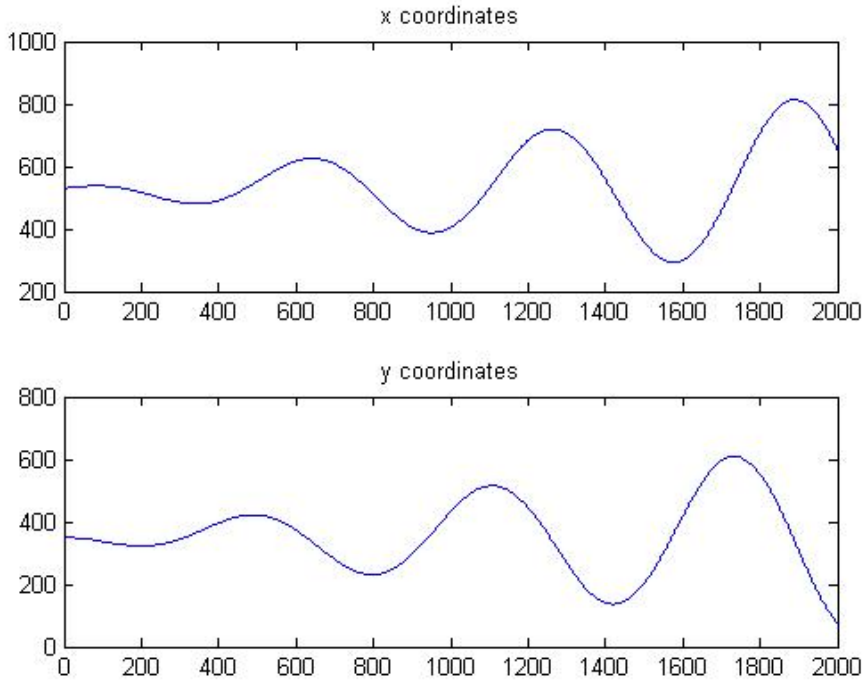

Figure II.1.2 Spiral1 generation mode, x and y coordinates display.

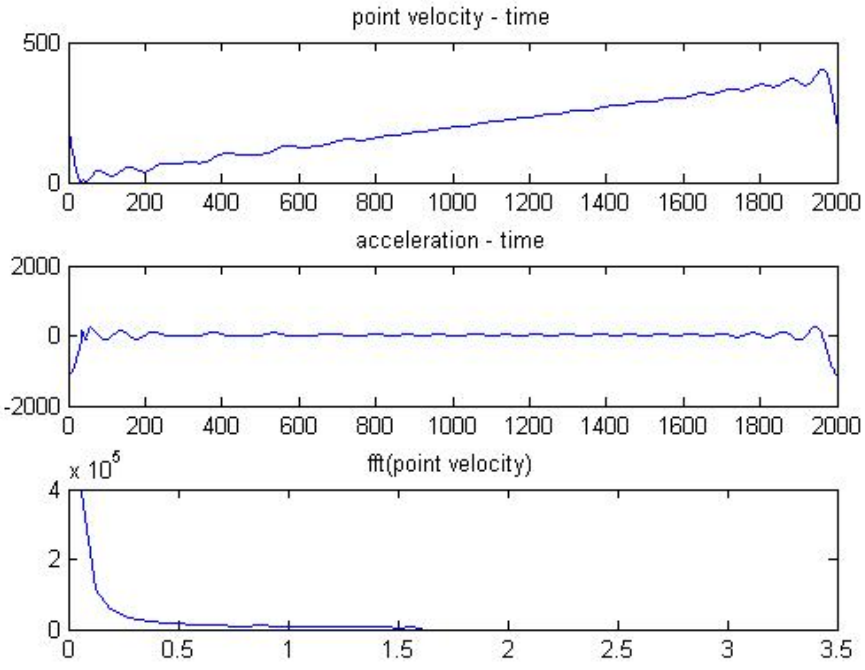

Figure II.1.3 Spiral1 generation mode, time domain information and frequency spectrum distribution.

b. Consistent linear velocity: Spiral2

In this case, the distance covered at each interval (arc between two adjacent points, *arc* = length of the spiral/*tp*) is a constant. Result in decreasing of increment $\Delta u(n)$while *n* increases because of increasing radius (radian = arc/ radius.)

When arc length is considerably small concerning the value of radius, radius changes in a very low rate, *r(n)* ≈ *r(n +1)*, therefore it is acceptable to use *r(n)* to substitute *r(n+1):*

$$\begin{aligned} radian(n+1) &= \frac{arc}{radius(n)} + radian(n) && n = 1...tp \\ radius(n) &= \sqrt{x(n)^2 + y(n)^2} && n = 1...tp \end{aligned} \tag{2.8}$$

Therefore

$$\begin{aligned} x(n+1) &= xc + amp(n) \times \cos\left(\frac{arc}{\sqrt{x(n)^2 + y(n)^2}} + radian(n)\right), && n = 1...tp \\ y(n+1) &= yc + amp(n) \times \sin\left(\frac{arc}{\sqrt{x(n)^2 + y(n)^2}} + radian(n)\right), && n = 1...tp \end{aligned} \tag{2.9}$$

When the trace of this equation match Spiral1,

$$\begin{aligned} x(n) &= xc + amp \times n \times \cos(\Delta u \times n), && n = 1...tp \\ y(n) &= yc + amp \times n \times \sin(\Delta u \times n), && n = 1...tp \end{aligned} \tag{2.10}$$

where $radian(n) = \Delta u \times n$. For the same spiral trace, points with the same radian have the same location coordinates, which means, when

$$\begin{aligned} radian(n) &= \Delta u \times n \\ &= \frac{arc}{\sqrt{x(n)^2 + y(n)^2}} + radian(n-1) \\ x(n) &= xc + amp \times n \times \cos(\Delta u \times n) \\ &= xc + amp(n) \times \cos\left(\frac{arc}{\sqrt{x(n)^2 + y(n)^2}} + radian(n-1)\right) \end{aligned} \tag{2.11}$$

therefore

$$
\begin{aligned}
amp(n) &= amp \times n \\
&= amp \times \frac{radian(n)}{\Delta u} \\
&= amp \times \frac{\frac{arc}{\sqrt{x(n)^2 + y(n)^2}} + radian(n-1)}{\Delta u} \qquad n = 1 \ldots tp
\end{aligned}
\tag{2.12}
$$

$$
(\Delta u = \frac{k\pi}{tp}, amp = \frac{radian}{tp}, \textit{ derivation detail see Spiral1})
$$

It is noted that *radian* represents the radians of the entire spiral, *radian(n)* is the radians of the *n*'s point since n = 0. *amp* is the amplitude gradient coefficient defined in Spiral1, *amp(n)* is the corresponding coefficient of the *n*'s point in Spiral2.

One issue of this mode is that at the very beginning of the spiral generation, radians and its increment are large because of small radius. The first couple of points would be considerably off the real spiral pattern in time domian. To solve this problem, the first 100 points are not generated via spiral2 but adopted from spiral1. Following data points are generated via spiral2 with radius [$x(100)^2+y(100)^2$]$^{1/2}$ to start with.

The following images are figures generated during the simulation of spiral under mode Spiral2. The velocity spectrum and acceleration spectrum show consistent characteristics with the assumptions.

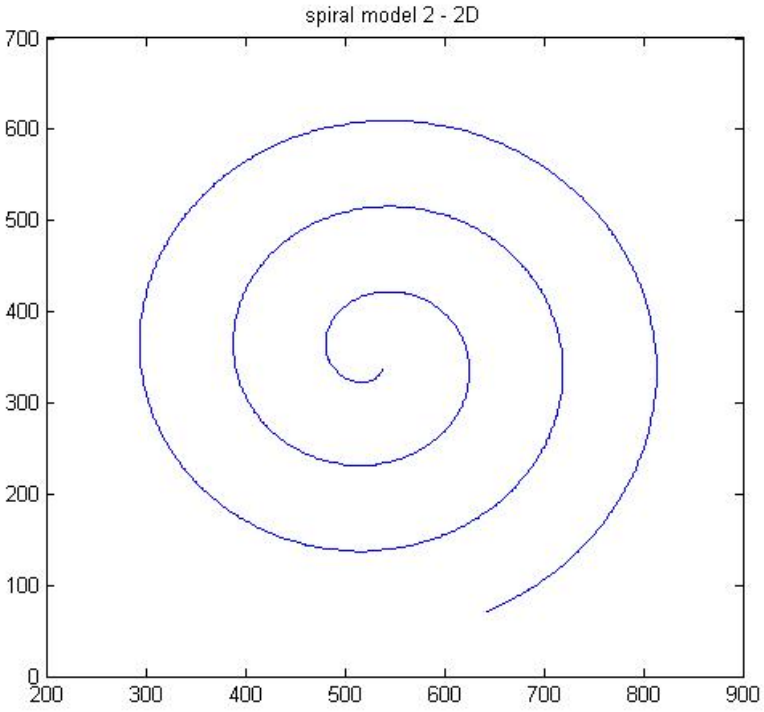

Figure II.1.4 Spiral2 generation mode, 2D final image.

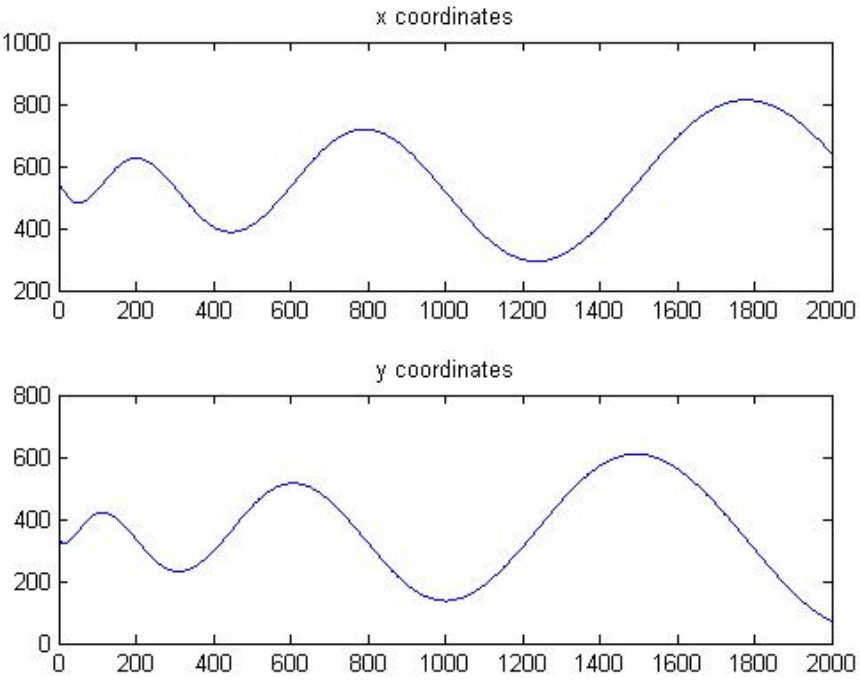

Figure II.1.5 Spiral2 generation mode, x and y coordinates.

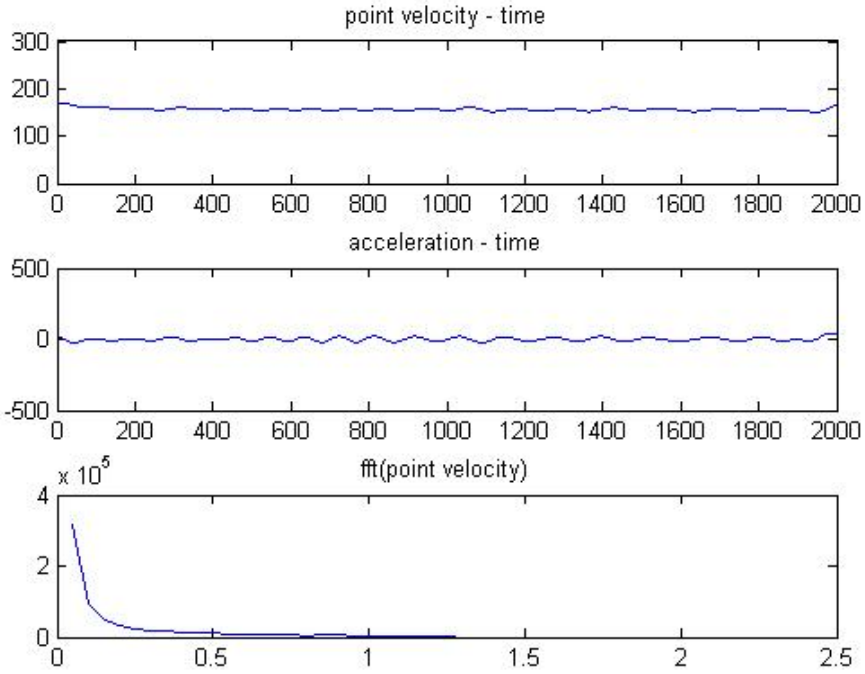

Figure II.1.6 Spiral2 generation mode, time domain information and frequency spectrum distribution.

1.2 Tremor Simulation:

Tremor simulation is in fact the simulation of series of oscillation movements. In this study, cosine/sine wave is applied as basic oscillation units in time domain. To initial this simulation, tremor pattern was extracted as a series of continuous bidirectional oscillation with a given range of frequency [*f1, f2*] at a given range of amplitude [*a1, a2*]. Accordingly, tremor simulation involves 6 parameters: minimum frequency *f1*, maximum frequency *f2*, minimum amplitude *a1*, maximum amplitude *a2*, recording duration indicator *tp* (timepoints, number of points recorded) and sampling frequency *sfreq* (in this study, 125Hz). We define this function as

tremor(*sfreq, tp, f1, f2, a1, a2*)

The method of generating a series of continuous cosine/sine waves with variation yet unbiased distribution in the range of frequency and amplitude is to generate and connect individual cosine wave unit with a randomly selected in frequency and amplitude within their defined ranges.

a. Basic unit:

Considering that cosine wave is symmetrical and that sine wave is Centro symmetric, wave of half wavelength is chosen as the smallest repeating unit. In the case of sine wave, the half wave always starts from $\sin(0) = 0$ and end at $\sin(\pi) = 0$. If half sine wave is applied as basic repeating unit in this simulation, the $\sin(k\pi)$ points would line up perfectly on x axis, which is less likely to be the case of essential tremor. In the case of cosine wave, the half wave starts from $\cos(0) =$ amplitude1 and ends at $\cos(\pi) =$ -amplitude2, or starts from $\cos(\pi) =$ -amplitude3 and ends at $\cos(2\pi) =$ ampulitude4. The points located at phase $k\pi + 0.5\pi$, that should align on x axis, would deviate from x axis when the amplitude of each unit starts to vary. This would result in a seemingly randomness in the resulting aggregation which reproduce a real tremor with better resembleness. For those two reasons, half cosine wave is applied as basic unit in this simulation.

b. Simulation Outcome:

To be consistent with the recorded data format and orgniation/arrangment, considering that tremor oscillation is along one axis, the outcome of tremor simulation should be an array of deviation distance in chronological sequence scanned at the sampling frequency.

c. Simulation Procedure:

Step 1. Calculate the maximum number of basic units possibly needed (equal to number

of peaks and nadirs minus one) by using *tp* and sampling point number of one cycle at the highest frequency possible *f*2. $\#units = 2 \times \frac{tp}{\frac{sfreq}{f2}} = 2 \times f2 \times \frac{tp}{sfreq}$.

Step 2. Define the turnning points of oscillation (peaks and nadirs) unit after unit. For each unit, a frequency and an amplitude are randomly selected. Except for the first unit where the amplitude of starting point is assigned to and the index of it is 1, every unit starts at where the last unit ends. The length (number of points) of this unit equals the nearest integer of $\frac{sfreq}{freq}$. The absolute value of the ending point (the last value of this unit in the outcome array) equals to the amplitude assigned to this unit, the value of the ending point is positive if the value of the ending point of the last unit is negetive, it is negative if the value of the ending point of the last unit is possitive.

Stpe 3. Fill the intervals between each turnning point with half—cycle cosine waves. For each interval, if it starts with a positive value and ends with a negative value, use cos([0, π]) to fill intervals, if it starts with a negative value and ends with a positive value, use cos([π,2π]) to fill the intervals. For each half-cycle cosine wave used for each paticuler interval, the amplitude of the wave equals half value of the difference bwteen the starting and ending values (amplitude is half value between the maximun and minimum), wavelength equals twice the length of its interval.

The following figure shows a simulated tremor during generation. The length of the tremor signal to be simulated is 2000 points. However during simulation, redundant turning points are calculated using maximum frequency, corresponding tremor sections

are generated (up to around 2300 points) to ensure sufficient length of the final output. Those extra points are cut off before passed on to the output variable.

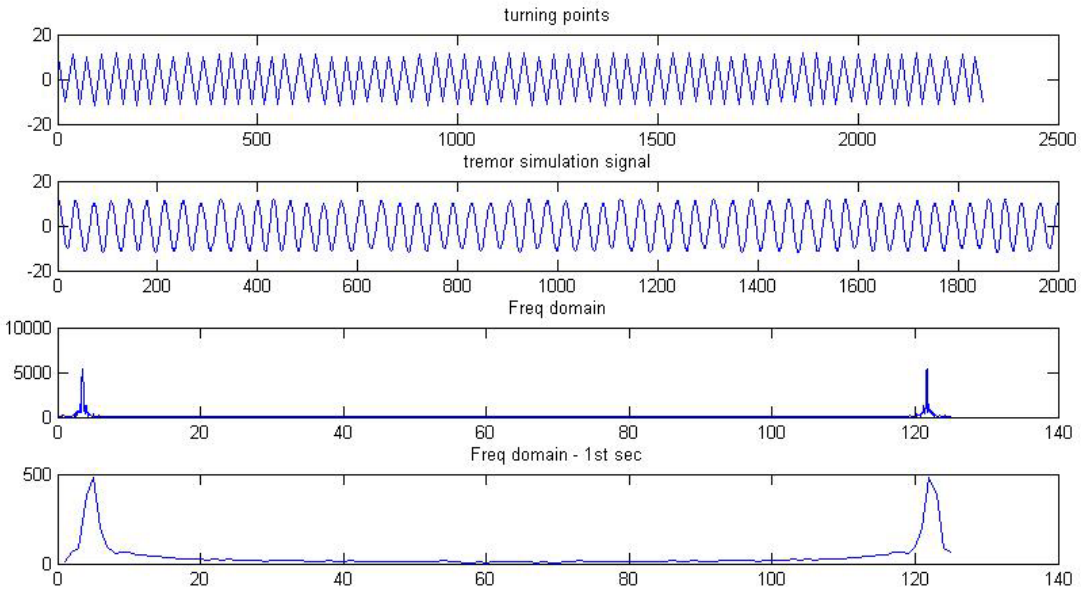

Figure II.1.7 Tremor durnning generation. The top fram shows the turnning points of the to be generated oscillation movement. The second fram shows the generated oscillation movement after filling each gaps between to turnning points with cosine waves. The third fram shows the frequency spectrum of the entire generated tremor signal. The bottom fram shows the frequency spectrum of the oscillation movement in the first second.

1.3 Spiral with Tremor Simulation:

Spiral with tremor is a spiral with a trermor patterned deviation at a certain angle, it is simply expressed as *spiral + tremor.* Spiral is composed by movement in *x* direction and movement in *y* direction,

spiral = spiral(x) +spiral(y)

Tremor is bidirectional, for one tremor, its axis has only one direction, and could be easily decomposed in to two movement in rectangular direction,

tremor = tremor(x) +tremor(y)

therefore

spiral with tremor =spiral(x) +spiral(y) +tremor(x) +tremor(y)

As discussed in Chapter I.4 study of interests the absolute angle (direction) of tremor with respect to the registration of model spiral is not crucial, to reduce the workload during simulation, considering that spiral with tremor at any direction can be achieved by rotation of spiral with tremor at a fixed direction, this simulation is downsized to the simpliest case, tremor direction is alinged with *x* axis or *y* axis,

spiralwithtremor =spiral (x) +spiral(y) +tremor(x)

or

spiralwithtremor = spiral(x) +spiral(y) +tremor(y)

in rectangular coordinates system expression:

$$\begin{aligned} spiralwithtremor(x) &= spiral(x) + tremor \\ spiralwithtremor(y) &= spiral(y) \end{aligned} \tag{2.13}$$

or

$$\begin{aligned} spiralwithtremor(x) &= spiral(x) \\ spiralwithtremor(y) &= spiral(y) + tremor \end{aligned} \tag{2.14}$$

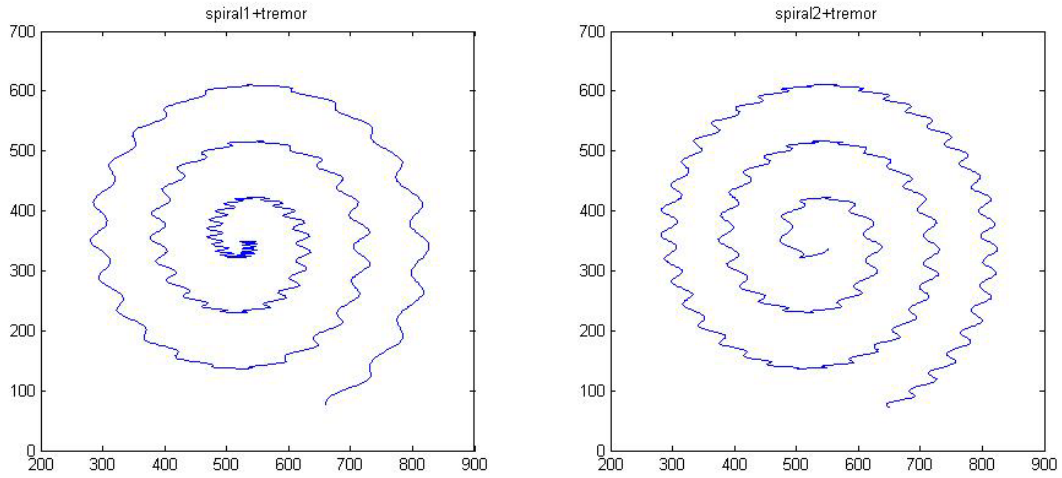

Figure II.1.8 Images of spiral tremor. On the left is a tremor spiral generated assuming drawing with consistent angular velocity along model spiral; on the right is a tremor spiral generated assuming drawing with consistent linear velocity along model spiral.

2. Pseudo Recording

Simulation data sets are algorithmically generated data series based on features extracted from actual patient recordings. To detect and exclude the unexpected differences in analysis performance caused by different data source, pseudo recordings were taken on the patient recording system by normal people (no tremor or any other movement impairing disease, right handed).

In general, two kinds of pseudo recordings were taken. The first one is smooth spiral recording for the calibration and alignment of standard spiral. The second one is spiral drawing with controlled consistent oscillations throughout the recording duration mimicking Essential Tremor symptom, yet highly regulated and ideal than a real patient recording. These pseudo recordings were used in the testing and adjustment of spatial domain and frequency domain processing related programs.

3. Patient Recording

Two databases were used in this study. One was used for exploring and evaluation analysis methods, the other was used to study the effects of alcohol and medication on the performance of Essential Tremor. Recording procedure for each individual is identical in each database. The only difference is that in the first database the recoding conditions and timeline relations between the same patient's recordings are not identified while in the second database those features are tagged for a grouped analysis.

To build the second database, the following experiment was conducted. 17 patients carrying diagnosis of Essential Tremor were asked to take spirography recordings through a period of time under three controlled conditions: a) no treatment (base line); b) under a stable dose of a beta-blocker named Inderal LA [propranolol SR (sustained release)] typically in the dose range of 60-120mg/day; c) immediately after intake of ethanol (40%, 50ml).

Two recordings of the same hand (right hand) under a same condition were taken at each visit. For each patient, baseline recordings were taken on the first visit. If the patient came back after Inderal treatment, a seconder set of recording was taken. Medication was suspended after the second recording. If the patient came back after the effect of medication ceased, the third set of ethanol-influenced recording was then taken. As the result, a group of 5 patients had all 3 sets of recordings, another group of 7 patients had the first 2 sets of recordings, and the last group of 6 patients had baseline recordings only were obtained.

At each recording, the patient was asked to sit upright on a chair. A tablet was placed on his/her lap horizontally. Then the patient was asked to draw a spiral on the tablet,

following the trace of a standard spiral displayed on the tablet screen. Throughout the recording, the patient was asked to keep his/her forearm parallel to horizon without any support.

Before analyzing the patient data, the algorithmic simulation data is first used because it has the best stability (in terms of noise level), and the outputs are expected (artificially and intentionally assigned when generating simulation data sets) so that the reliability of the tested algorithm could be examined. Pseudo recordings are then applied to test the performance of processing data from the real recording system, because the pseudo recording data is ideal and distinctively characterized by a normal subject's control. Only after the algorithm is proven feasible, stable and reliable by the first two categories of data sets, should the real patient recordings be processed for comprehensive report.

Chapter III: Frequency Domain Analysis

The raw data stored in recording files are location coordinates in chorological sequence. Its first order differentiation times sampling frequency results in the instantaneous velocity with respect to time, i.e., time domain spectrum**.** With Fast Fourier Transformation (FFT), frequency spectrum can be obtained. This is the main procedure of all frequency domain analysis, the differences between methods used in each individual studies lay in the choice of coordinate system, preprocessing of raw data and post FFT processing.

Considering that the intended movement (trace) of spirography drawing is a smooth spiral (the Archimedean spiral model), which has a constant and continuous change in its tangential direction (instantaneous velocity direction), in this study, processing of instantaneous velocity were executed and compared in both rectangular coordinate system and polar coordinate system.

In this location-velocity-frequency processing, locations of recorded points are first transformed into distance between adjacent points. The distance between two known points is a fixed value in spite of the orientation of coordinate system. Therefore the difference of the recording rectangular coordinate system orientation and the mapping rectangular coordinate system orientation does not affect the results if it is uncounted for. To simplify the process, the orientation disagreement is ignored in FD analysis.

1. Trial 1: Processing in Rectangular Coordinate System

Procedure:

1. Read data into array *x* (*x* coordinate of each point) and array *y* (*y* coordinate of each point). Count the number of elements in either array (dimensions of *x* and *y* should match) as *tp*.
2. Calculate the distance between each adjacent points

$$\begin{aligned} &dis(n) = \sqrt{[x(n)-x(n-1)]^2 + [y(n)-y(n-1)]^2} && n = 2...tp \\ &dis(1) = 0 \end{aligned} \tag{3.1}$$

   n is the index of each point, $n \times sfreq$ is the time of recording of each point with respect to the starting point. Hence the *n vs. dis* is equivalent to *time vs. dis*.

3. Calculate the instantaneous velocity and acceleration of each point (each sampling time)

$$\begin{aligned} &v(n) = dis(n) \times sfreq, && n = 1...tp \\ &acc(n) = (v(n)-v(n-1)) \times sfreq, && n = 1...tp \end{aligned} \tag{3.2}$$

4. Conduct FFT on *v* and *acc*, get frequency spectrum *fft_v* and *fft_acc*

$$\begin{aligned} &fft\_v = fft(v) \\ &fft\_acc = fft(acc) \end{aligned} \tag{3.3}$$

In frequency domain, the outcome array has the same dimension as the input array, *tp*. Like the index-time conversion in the cases of time domain parameters, an index-frequency conversion is necessary for the identifying of interested region in frequency spectrum. No matter how long the raw data (recording duration) is, the upper limit of the frequency of which information could be recorded is the sampling frequency. Therefore the highest frequency in the frequency spectrum (the last element of the outcome array, index $n = tp$) matches sampling frequency (*sfreq=125*Hz). Because the highest frequency

that contain information from any kind of original data is half the value of the sampling frequency, the frequency of spirography information actually recorded ranges from 0 to 62.5 Hz. The conversion from index *n* to actual frequency is linear scaling,

$$actual\_frequency(n) = n \times \frac{sfreq}{tp} \tag{3.4}$$

The accuracy of this conversion is confirmed by counting the number of cycles within one second in time domain.

2. Trial 2: Processing in Polar Coordinate System

Procedure:

1. Read data into arrays *x* (*x* coordinate of each point) and array *y* (*y* coordinate of each point). Count the number of elements in either array (dimensions of *x* and *y* should match) as *tp*.
2. Transform rectangular coordinates into polar coordinates.

$$\begin{aligned} \rho(n) &= \sqrt{x(n)^2 + y(n)^2} \\ \theta(n) &= \tan^{-1}\left(\frac{y(n)}{x(n)}\right) \end{aligned} \tag{3.5}$$

   ρ is the distance to the center (the first point of model spiral), θ is the angle from (1,0) vector.

3. Calculate the distance between each adjacent point

$$\begin{aligned} dis(n) &= |\rho(n) - \rho(n-1)| \qquad n = 2...tp \\ dis(1) &= 0 \end{aligned} \tag{3.6}$$

4. Calculate the instantaneous velocity and acceleration of each point. This is the same as Procedure 3 in rectangular coordinate system based approach.

5. Conduct FFT on *v* and *acc*, get frequency spectrum *fft_v* and *fft_acc*. This is the same as Procedure 4 in rectangular coordinate system based approach.

3. Results And Comparison

In the following demonstration, the parameters of simulated data were set up as follows:

sfreq = 125 Hz

tp = 2000

min(frequency) = 4 Hz

max(frequency) = 5 Hz

min(amplitude) = 10 pixel = 2.5 mm

max(amplitude) = 14 pixel = 3.5 mm

Tremor1 is spiral generated via Spiral1 with tremor oscillation along *x* axis (horizontal).

Tremor2 is spiral generated via Spiral2 with tremor oscillation along *x* axis.

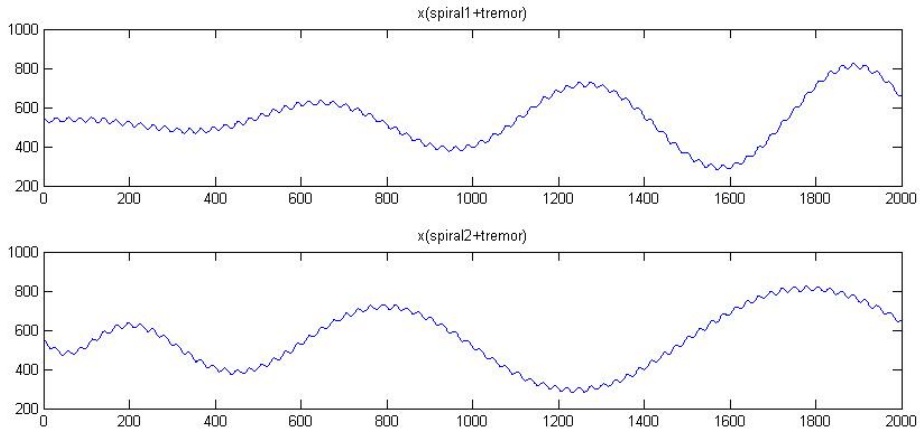

Figure III.3.1 Value of x coordinates through time (coordinate vs tp). The figure in the upper frame is x(n) of tremor1, the figure in the lower frame is x(n) of tremor2. y(n) of both tremor1 and tremor2 are the same as its component spiral, as shown in Chapter II.

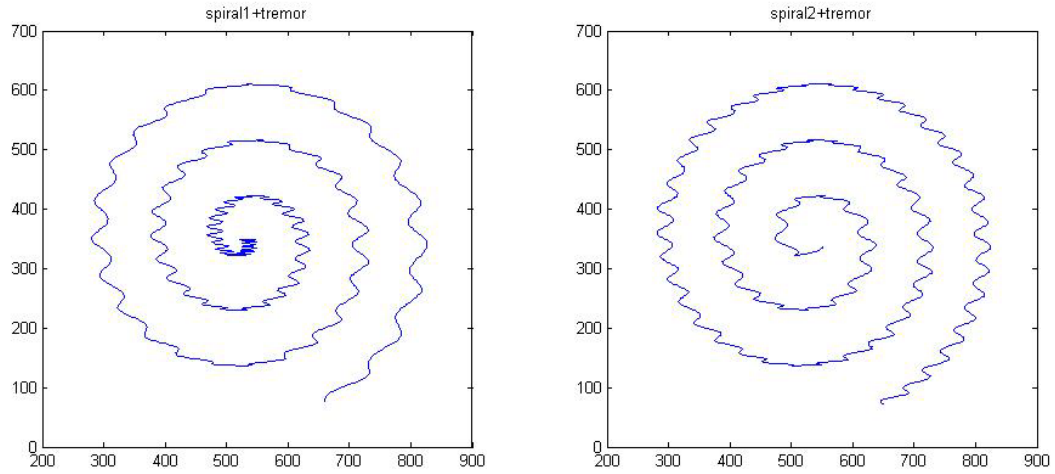

Figure III.3.2 Tremor1 and tremor2 in spatial domain.

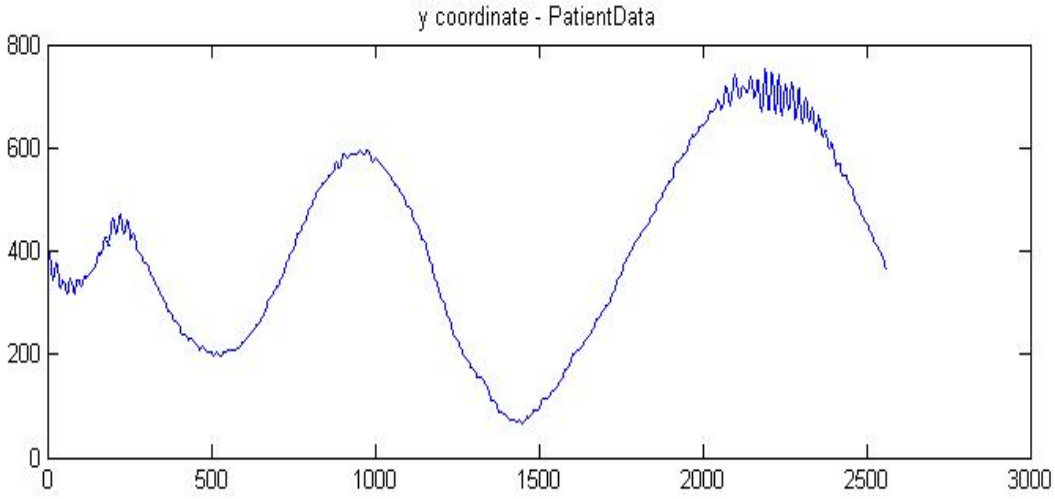

Figure III.3.3 Patient recording – y coordinate. This shows the value of y coordinates through time (tremor oscillation axis align with y axis better than with x axis).

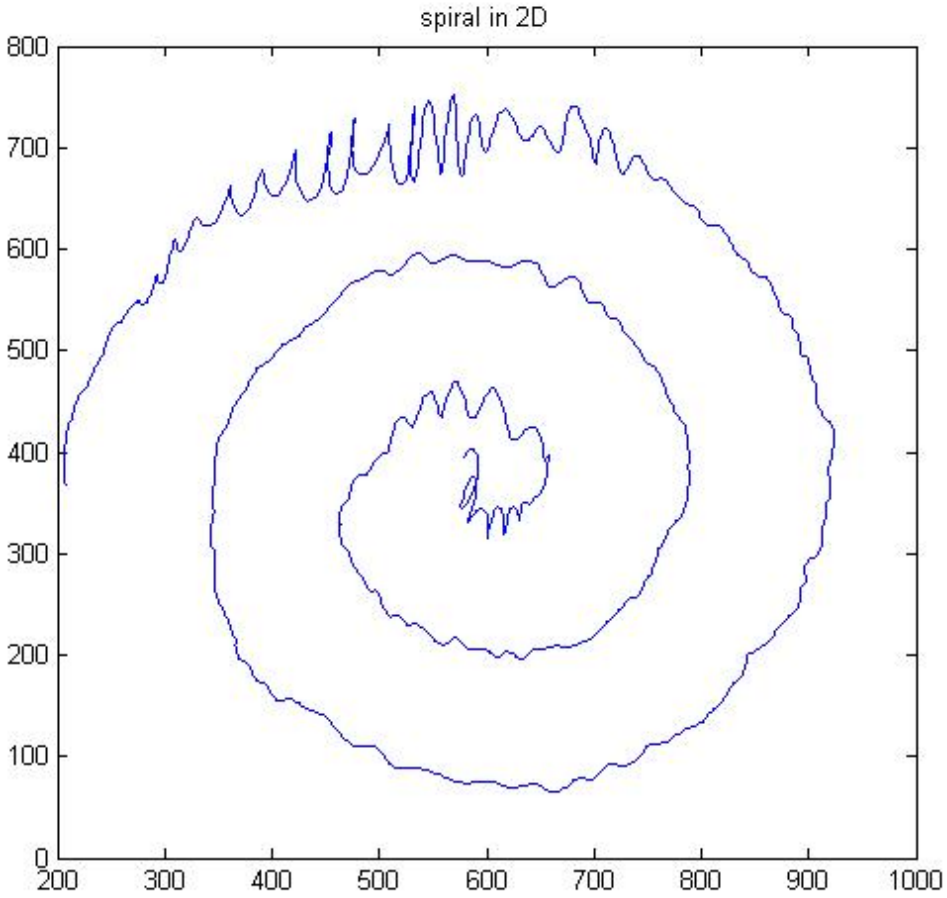

Figure III.3.4 Patient recording. This shows the final image drawn (spatial domain).

According to these images, we can conclude that Spiral2 resembles tremor patient recording with higher identicalness (the wavelength of each oscillation unit does not vary with their responding locations.) This is consistent with the understanding that people tend to draw lines with a steady linear velocity.

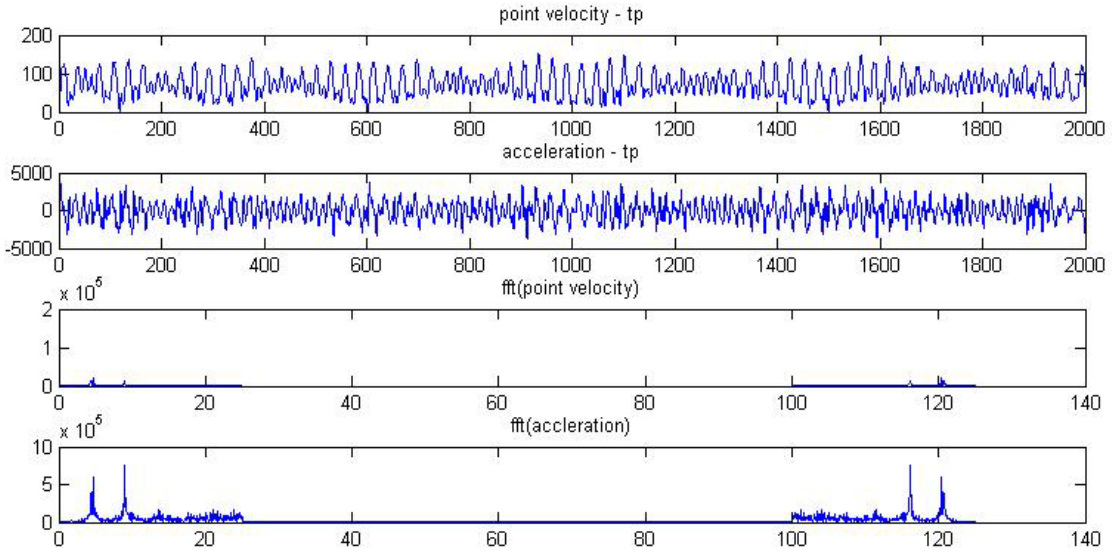

Figure III.3.5 Trial 1 processing of tremor2. The velocity frequency spectrum in this figure was 25 Hz low pass filtered to eliminate high frequency noise integrated due to sampling and digitizing before acceleration was calculated, hence in frequency spectrum of velocity and acceleration information only exist between 0~25 Hz. Frequency of the first peak is around 4.4 Hz, frequency of the second peak is around 9 Hz.

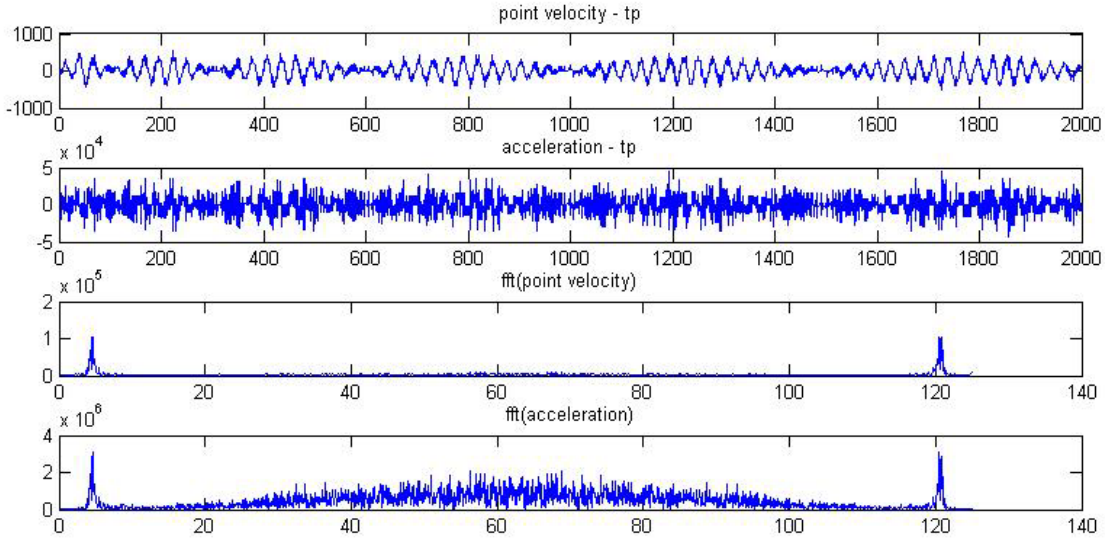

Figure III.3.6 Trial 2 processing of tremor2. Frequency of the peak is around 5 Hz.

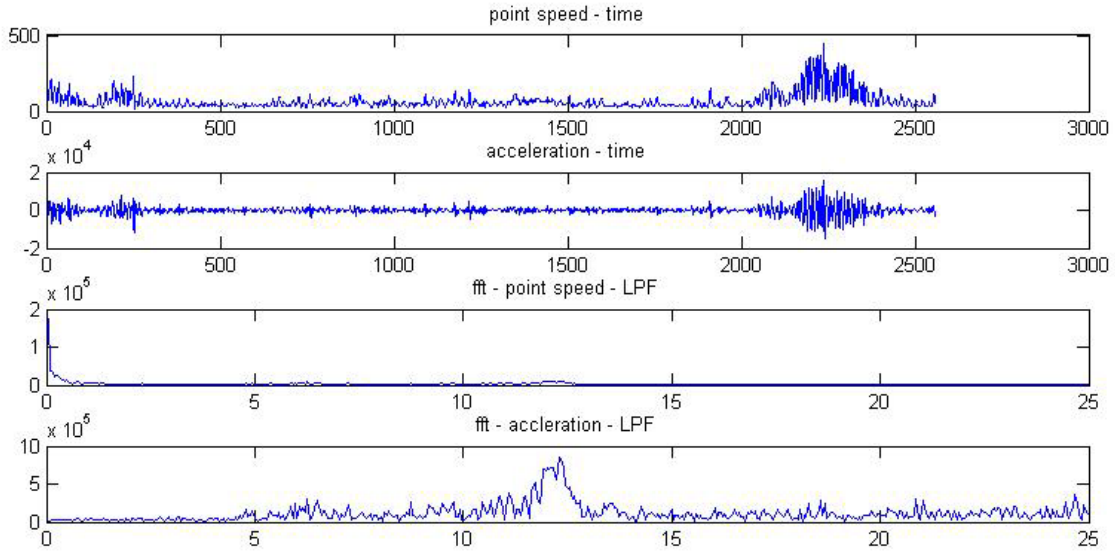

Figure III.3.7 Trial 1 processing of patient recording. The velocity frequency spectrum in this figure was 25 Hz low pass filtered to eliminate high frequency noise integrated due to sampling and digitizing before acceleration was calculated, hence in frequency spectrum of velocity and acceleration information only exist between 0~25 Hz. Frequency of the largest peak is around 12.5 Hz.

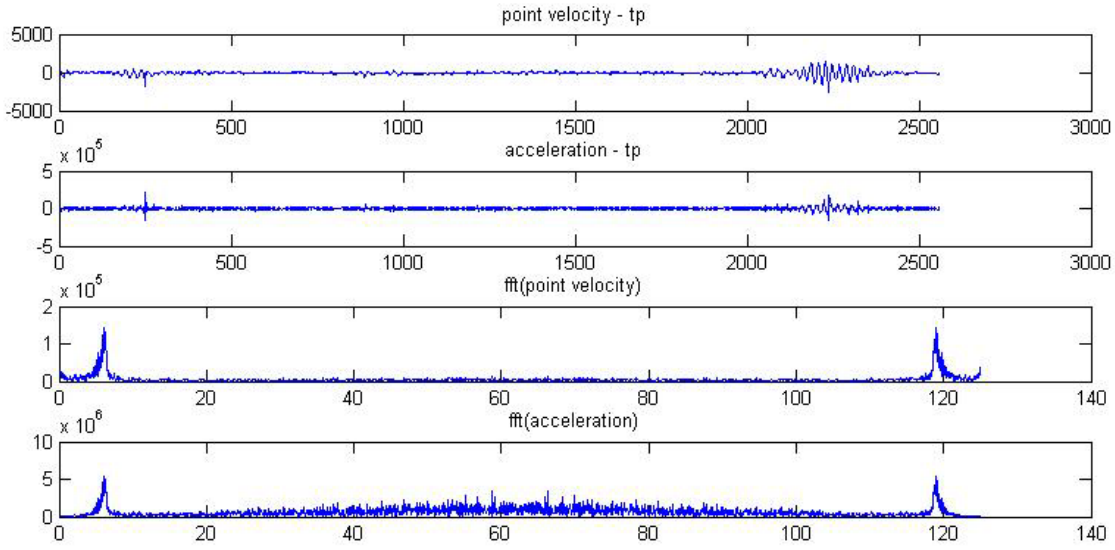

Figure III.3.8 Trial 2 processing of patient recording. Frequency of the peak on the left is around 6Hz.

It can be seen from these figures that in spite of differences in time domain, the frequency spectrum distribution of velocity and acceleration are similar, the values increase and decrease in a synchronized manner. This synchronization in simulation data could be explained as the result of application of cosine wave as basic unit (Chapter II.1):

For any cosine wave in spatial domain $s = A \times \cos(b\pi + c)$, the equation of its velocity in time domain is its first order differentiation $v = B \times \cos(b'\pi + c' + 0.5\pi)$, *b'* and *c'* stands for the frequency change after conversion take in account of scanning frequency. Acceleration is first order differentiation of velocity $acc = C \times \cos(b'\pi + c' + \pi)$. From velocity to acceleration, the phase of the wave has a 0.5π shift during differenciaion, but the frequency stays unchanged *b'*. For a series/collection of cosine waves with certain distribution of frequencies, the frequency of each cosine wave unit does not change during differentiation but only with certain phase shift in a synchronized manner, therefore the distribution of frequency does not change.

Spatial Domain wave function:

$$f(n) = \Sigma a_n \times \cos(\omega_n \pi + \theta_n) \tag{3.7}$$

Time Domain, velocity function:

$$\begin{aligned} v(n) &= sfreq \times (f(n) - f(n-1)) \\ &= sfreq \times \Sigma a_n \times \cos(\omega_n \pi + \theta_n + 0.5\pi) \end{aligned} \tag{3.8}$$

Time Domain, acceleration function:

$$\begin{aligned} acc(n) &= sfreq \times (v(n) - v(n-1)) \\ &= sfreq^2 \times \Sigma a_n \times \cos(\omega_n \pi + \theta_n + \pi) \end{aligned} \tag{3.9}$$

3.1 Issue: Frequency Doubling

However, one issue raised during processing is that instead of using first order differentiation of the spatial domain wave function owing to its unknown value, distance travelled per unit time is applied to find velocity function. Distance between two points is a positive value that has no direction, as the result, the negative part of a cosine wave would flip to its absolute value. Consequently, frequency would turn out doubled during this process.

The following figures are demonstrations of the frequency doubling phenomena via simulation data.

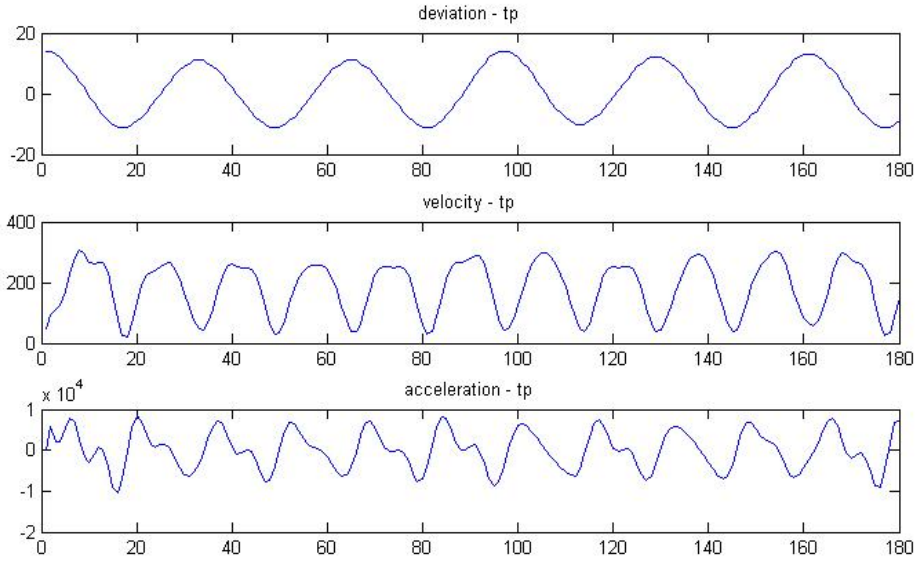

Figure III.3.9 Frequency doubling phenomena in time domain. On the top shows the deviation according to time, movement direction is either towards positive or negative. In the middle frame is velocity display, the frequency doubling due to absolute value extraction could be clearly seen. In the bottom frame is the acceleration display, its frequency is accordingly doubled along with velocity.

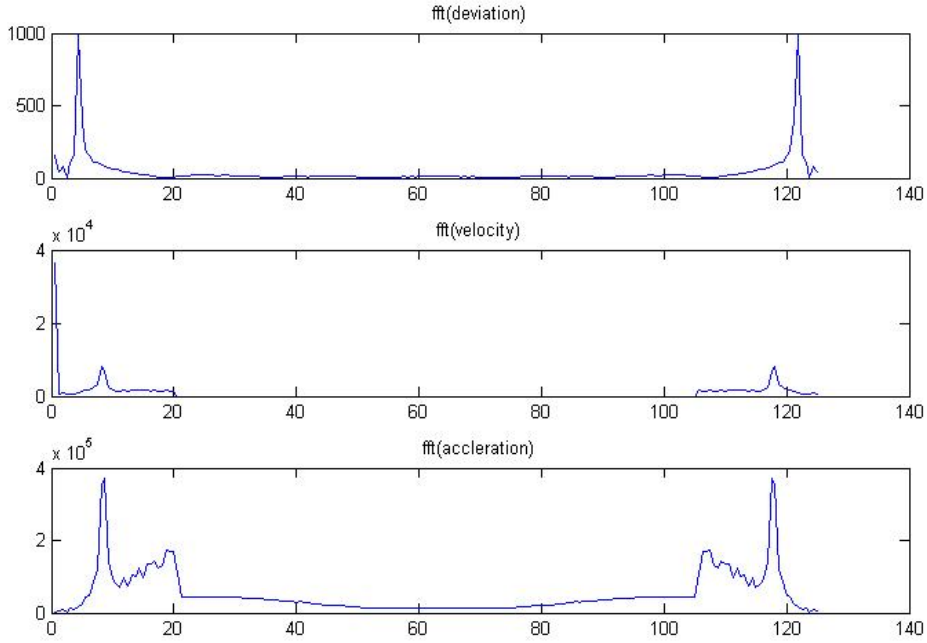

Figure III.3.10 Frequency doubling phenomena in frequency domain. Peak frequency is 4.375 Hz in the top frame which is the frequency spectrum of a simulated tremor deviation signal, 8.7 Hz in the middle frame, 8.7 Hz in the bottom frame. Low pass filter at 20 Hz.

Frequency doubling only occurs once during location-velocity translation. Therefore frequency spectrum of velocity and acceleration still maintain their synchronization. The consistency of this synchronization in frequency spectrum of velocity and acceleration shown in the results of patient recording confirmed the plausibility of using cosine wave as basic unit in simulation.

3.2 Dominant Frequency Identification

In the frequency spectrum of simulated data in *Figure III.3.5*, 2 apparent peaks can be identified. Meanwhile in *Figure III.3.7,* in the case of patient recording, such pattern could also be observed. The first peak is believed to be the residue of original waveform

before predominant frequency doubling. The corresponding frequency has exactly half the value of the second peak. The second peak is confirmed as the dominant frequency (DF) by counting the number of wave cycles in time domain. Considering the frequency doubling, (the second peak is the real DF peak of absolute instantaneous velocity while the reading of the first peak equals to the DF of oscillation movement) the resulting predominant frequency of simulation data shows consistency with its setup.

3.3 Comparison: Trial 1 and Trial 2

To compare the outcome of trial 1 and trial 2, the following experiment were conducted:

Tremor1=Spiral1(125, 2000) + tremor(4,5,6,9)

Tremor2=Spiral2(125, 2000) + tremor(4,5,6,9)
*sampling frequency 125Hz, tp = 2000, frequency 4~5 Hz, oscillation amplitude 6~9 pixel.

In the resulting frequency spectrum, there are two apparent peaks in trial 1 (peaks before and after frequency doubling,) yet for trial 2 there's only one primary peak, the second primary peak does not exist because of the algorithm used to find instantaneous velocity is based on differentiation of location (radius of each points in polar coordinate system) instead of distance between adjacent points, therefore no frequency doubling, no second primary peak (see *Figure III.3.5* and *Figure III.3.7*.)

In spite of the missing of the second peak in trial 2, there are subtle differences between the first peak of the two trials: trial 2 has more details in the first peak region - the residue region. The following table shows the readings from the first peak region. Peak 1-1 stands for the first summit in the first peak region, peak 1- 0 is the summit before that. Not all spectrums have Peak 1-0.

		Tremor1		Tremor2	
		Trial 1	Trial 2	Trial 1	Trial 2
Velocity frequency spectrum	Peak 1-0	-	4.25	-	4.188
	Peak 1-1	4.375	4.375	4.313	4.313
	Peak 1-2	4.688	4.688	4.75	4.75
Acceleration frequency spectrum	Peak 1-0	-	-	-	-
	Peak 1-1	4.375	4.375	4.313	4.313
	Peak 1-2	4.688	4.688	4.75	4.688

Table III.3.1 Trial 1 and Trial 2 result of simulation data.

The table shows that the readings in acceleration frequency spectrum are consistent between trial 1 and trial 2, except for peak 1-2 of Tremor2. In the velocity frequency spectrum, the extra summit peak 1-0 of trial 2 could be the result of polar coordinate system translation. The continuous status change of alignment between recorded movement direction and coordinate system direction could lead to bandwidth broadening, hence one more summit in spectrum details in the front.

In general, trial 1 is preferred better that trial 2 because of the bandwidth broadening of primary peak in which would in turn influent the final readings.

Chapter IV: Spatial Domain Analysis

The purpose of spatial domain analysis is to unwrap the spiral drawing to see if there is a pattern that can quantitatively identify the amplitude of tremor (involuntary movement).

1. Trial 3: Unwrapping the Spiral

The first attempt to identify the amplitude of tremor is the unwrapping of the spiral. The idea comes from coordinate system transformation in trial 2 where the rectangular coordinate (x,y) are transformed into the polar coordinate (ρ,θ), then displayed data in the ρ-θ plan.

In the transformation, according to equation $\theta = \tan^{-1}(\frac{y}{x})$, the range of θ is restrained to $[-\frac{1}{2}\pi,+\frac{1}{2}\pi]$ while the radian covered by the spiral goes far beyond $\frac{1}{2}\pi$, reaching as much as 6π. This range restriction results in the break down and over lapping/superposition of ρ value every 180 degree. However this could be adjusted by extracting the characteristics before and after the "leaping".

Figure IV.1.1 displays the unwrapping of a model spiral and a simulated tremor spiral, radians ranges have been adjusted. Both model spiral and tremor spiral are for the recording of the right hand, therefore the drawing is counterclockwise, resulting the range of radian goes from around -2.5 rad to around -20 rad.

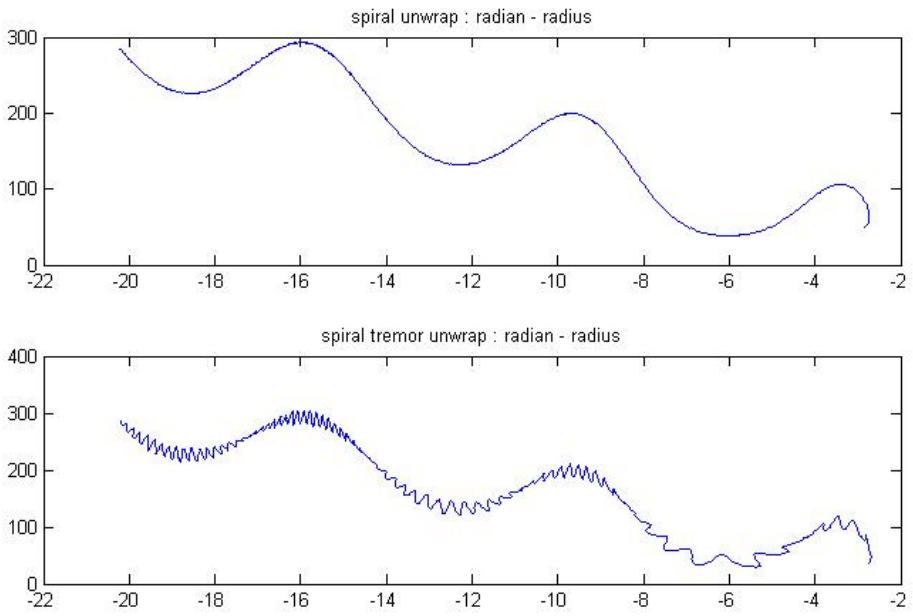

Figure IV.1.1 Unwrapping the spiral via coordinate system transformation. Radians range adjusted. In the upper frame is the unwrapping of a smooth/model spiral, in the lower frame is the unwrapping of a tremor spiral.

The unwrapped spiral displays a pattern of interrupted zigzag waves with the direction of sawtooth change continuously. This is because between radian 0 and radian 2π, the direction of radius is continuously changing, while the direction of tremor remains the same roughly. This results in the alteration of alignment and phasing off of these two direction vectors. The sawtooth "stand up right" when the two vectors are well aligned, "lean to either side" when they phase off, "vanish" (straight section, interruptions) when they are in an orthogonal position.

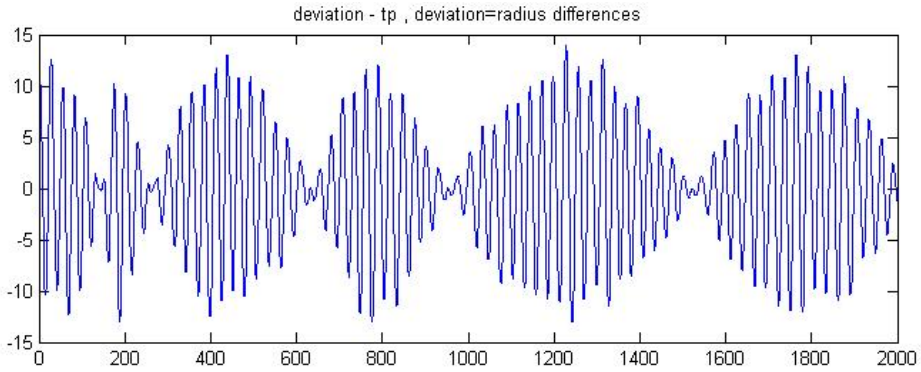

Figure IV.1.2 Tremor trace obtained from unwrapping. Tremor trace = tremor unwrapped – spiral unwrapped.

This fine pattern displayed in *Figure IV.1.2* only exists in simulations when the unwrapped tremor spiral and model spiral are perfectly aligned by their index number, which is the angle of each point. In reality, no one can draw spiral under constant velocity as precisely as clockwork, which would lead to misalignment of unwrapped tremor spiral and unwrapped model spiral. This means parameters of unrelated points are compared, which in turn would lead to irregularity of the resulting figure.

Even in the perfect scenario of simulated data, such as the result in *Figure IV.1.2*, we can see that it is still not easy to identify and calculate tremor amplitude by this unwrapping method. Looking at the tremor in the perspective of spiral does not give a satisfying result, but it introduces the idea of looking at the spiral in the perspective of tremor, which is the guiding idea of trial 4.

2. Trial 4: Tremor Amplitude Quantification

We have demonstrated in the simulation experiment and observed from the patient recording data that spiral drawing is the integration of spiral (voluntary) and tremor (involuntary) movement. Based on the definition, tremor trace in spatial domain could be

obtained by isolating the amplitude of model spiral from the amplitude of combined movement at the direction of tremor oscillation axis.

Figure IV.2.1 demonstrates the relationships of model spiral, tremor spiral, tremor oscillation direction and tremor deviation.

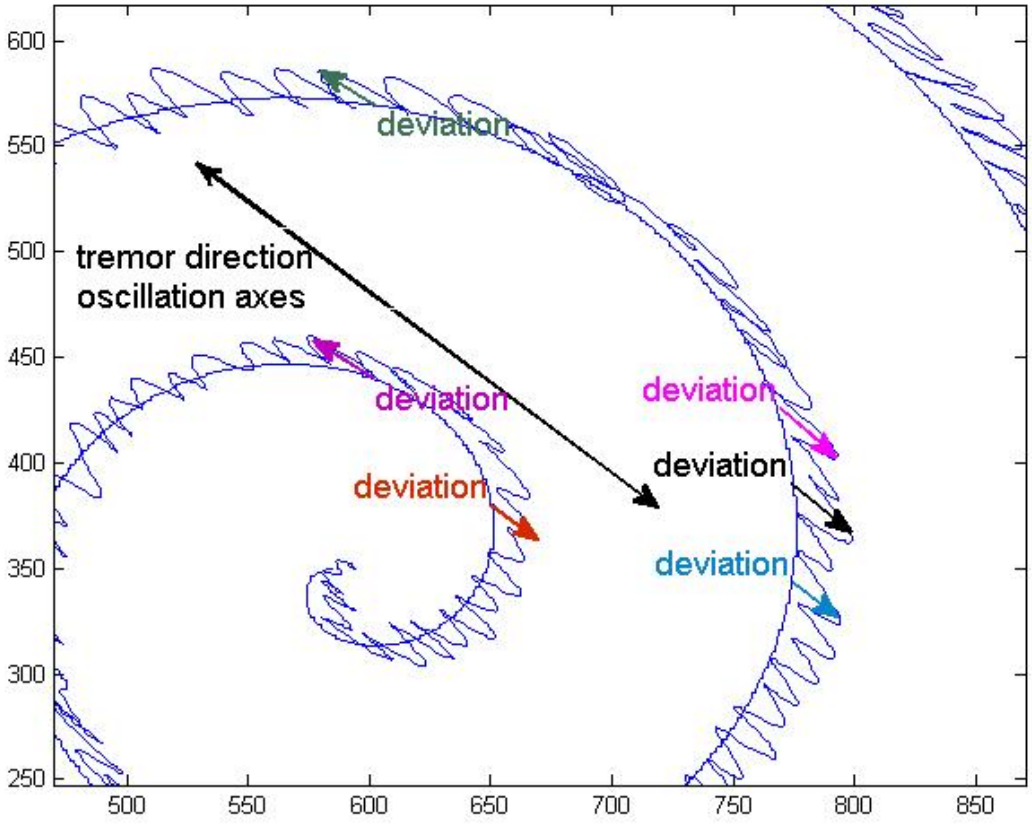

Figure IV.2.1 Deviation demonstration

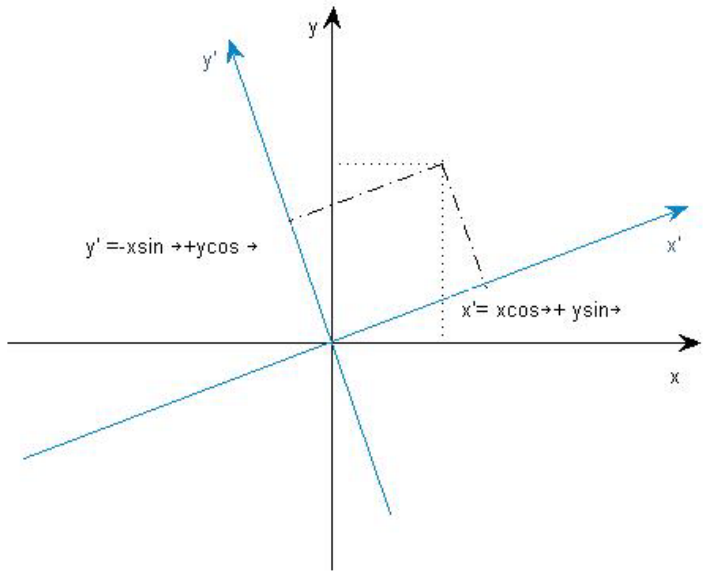

Figure IV.2.2 Angular coordinate system transform

Figure IV.2.2 is a demonstration of Angular coordinate system transformation. The *x-y* coordinate is the original rectangular coordinate system, which is used in recording and raw data reading. The *x'-y'* coordinate is the rectangular coordinate system after transformation according to the characteristic angle of tremor. If the angle from *x-y* to *x'-y'* is α,

$$\begin{aligned} x' &= x\cos\alpha + y\sin\alpha \\ y' &= -x\sin\alpha + y\cos\alpha \end{aligned} \tag{4.1}$$

For each point of the tremor spiral, there is a corresponding point on the model spiral. In the *x'-y'* coordinate system, these corresponding points share a same *x'* coordinate, their *y'* coordinate difference is the amplitude of the corresponding point of the isolated tremor (value of the deviation),

$$d = y'(tremorspiral) - y'(modelspiral) \tag{4.2}$$

In this manner, tremor along a model spiral is unwrapped into " tremor space" along a straight line. The movement along the line is the voluntary movement. The movement orthogonal to the straight line is the involuntary oscillation.

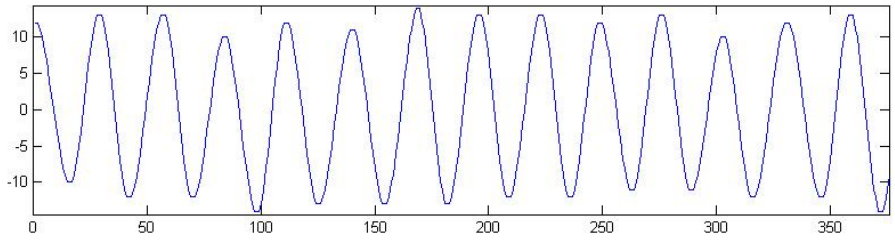

Figure IV.2.3 Unwrapped tremor. Values on y axis stand for deviation from the intended trace, unit in pixel.

Amplitude of tremor oscillation does not change abruptly. Therefore to identify and quantify this tremor amplitude, any portion including at least 4 full cycle oscillation is sufficient to represent the whole recording. The benefit of this representation is an optimized procedure and considerably reduced processing load.

Procedure:

Step 1. Identify tremor direction. In this study, radon transform is used to quantitatively identify the angle of tremor. Radon transform is integral transform consisting of the integral of a function over straight lines. It is projections of image along each angle. Radon transform results in a matrix with 180 columns. The index of each column indicates angle from 0 degree to 179 degree respectively. 1 degree increment of angle is used in the study, but it could be any other amount as needed. The data in each column is the projection profile of the image at its corresponding angle.

Figure IV.2.4 Radon domain of a simulation data

In the radon domain, the "image" intensity is the summation of transformed image along certain direction by the column index. A region/pixel with high intensity value distinguished from its background neighborhood indicates the texture of the original image has a lot line tracks aligned in the angle indexed by the column number. Together with restriction conditions, radon transform is applied in order to quantify tremor angle.

Step 2. Angular adjustment – rotation of the image along with model spiral

Instead of transforming coordinates for each point recorded in chorological sequence, a rotation of the 2-dimentional images of the recording and model spiral could also result in

the vertical alignment of corresponding points on tremor spiral and model spiral according to the angle of interest. The result of the rotated image is equivocal to the image of coordinates after angular translation.

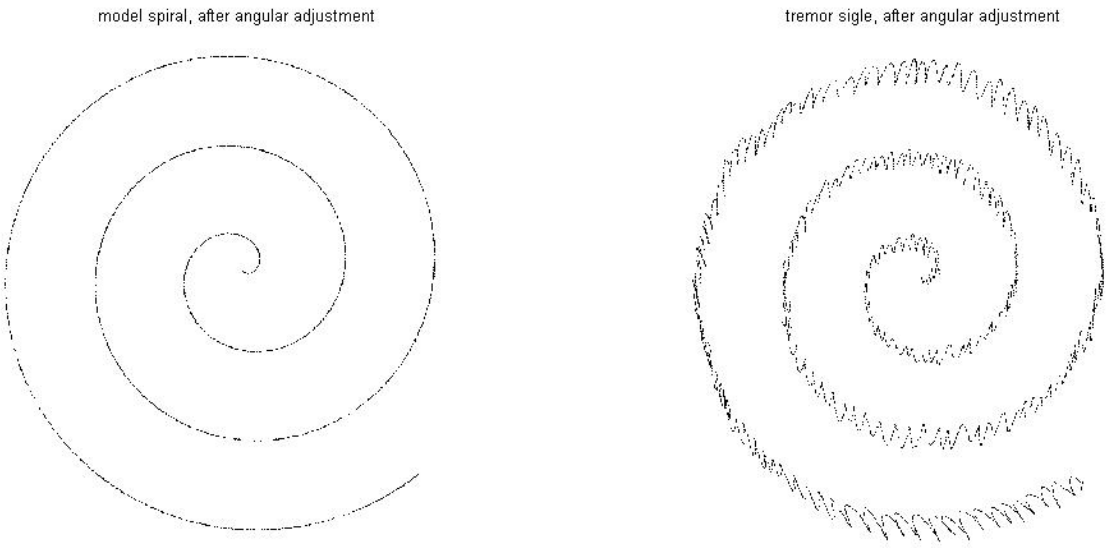

Figure IV.2.5 Angular adjusted tremor-spiral and model spiral

Step 3. Choose a section of the image that displays the deviation between tremor-spiral and model spiral best. As shown in *Figure IV.2.1*, because of the align-phase off-orthogonal of the tremor direction and spiral direction, some portion of the tremor oscillation are so intensely squeezed that each wave could hardly be distinguished from its adjacent wave.

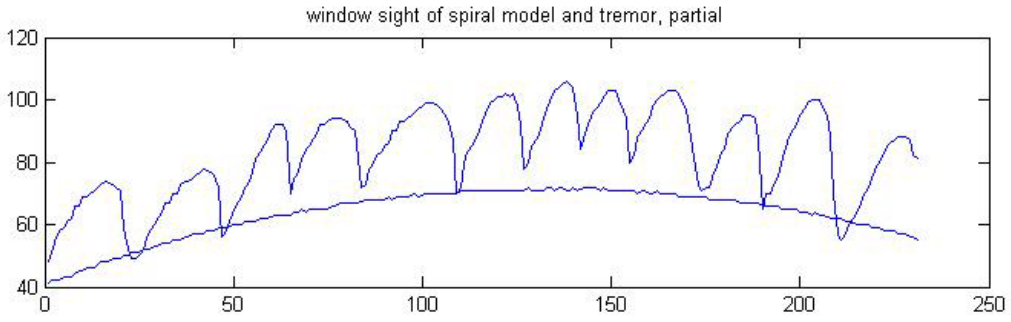

Figure IV.2.6 Window view

In general, the portions between -30 and 30 degree to vertical is preferable. At the same time, apparent disturbance in the voluntary movement (large deviate from tremor axes to model spiral) should be avoided.

Step 4. Quantification and subtraction. In step 2, the data under processing has been transformed from coordinate pairs (array *x,* array *y*) into image (2 dimensional matrix). Step 3 results in 2 matrixes with the same dimensions from tremor spiral and model spiral respectively. To quantify the deviation of the 2 lines in these images with concern of direction, the matrixes needs to be translated in to (*x,y*) coordinates and match up before comparison. The result of this subtraction is an array of positive and negative numbers presenting the value of deviation. It is the isolated tremor trace.

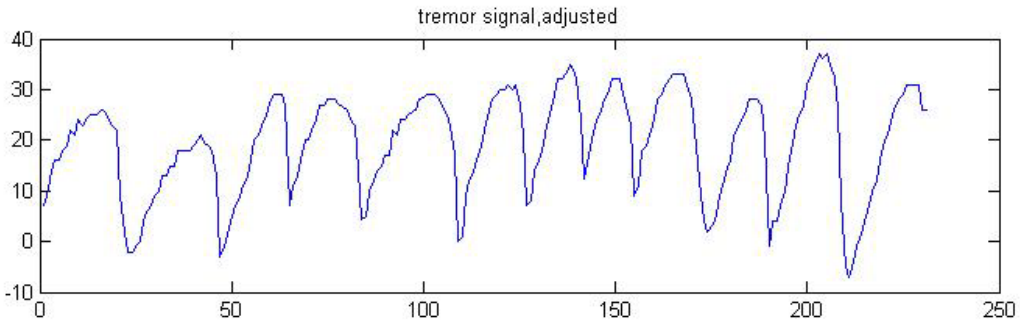

Figure IV.2.7 Tremor signal (partial)

Step 5. Amplitude extraction. At this point, the amplitude of tremor could either be read from display manually, or under certain transformation be extracted via computational processing automatically.

Chapter V: Discussion and Conclusion

1. Database Processing

The purpose of DataBase1 is mainly to exam and tune the developed algorithm and to obtain some general observations and confirmation of early assumptions:

a. In Essential Tremor cases, kinetic tremor on hand could be bilateral or unilateral.
b. Tremor frequency is stable in short term. Predominant oscillation frequencies of Essential Tremor mostly range between 3~8 Hz, oscillation amplitude varies from case to case.
c. The majority of Essential Tremor cases have only one tremor direction. Only in rare cases does a second tremor direction exist.

The statistics of the processing results of DataBase1aggrees with these assumptions. In the debate of tremor oscillation frequency range, the range 3~8Hz does not conflict with the 8~12 Hz range stated in the introduction section of this thesis when frequency doubling is accounted for.

The purpose of collecting DataBase2 is to quantitatively compare the influence of alcohol and Inderal. Unfortunately because of the lack of applicable patient recording, no conclusion could be draw at this point. 67 recordings from 17 patients were collected, 45 of which have oscillation amplitude smaller than 0.5mm and were recognized as non-tremor recording not applicable for further analysis. Among the remaining recordings, Patient 02, Patient 06 and Patient 13 are the only ones have plausible baseline and Inderal recordings, others only have tremor recording under one condition, mostly baseline. Patient 02 and Patient 13 show slight DF decrease under influence of Inderal, Patient 06

shows slight increase in DF which could be the result of unaccounted recording environment influences.

2. Frequency Analysis: Deviation, Velocity or Acceleration

In this study, frequency analysis of velocity and acceleration was applied. As a result of the deviation-velocity (absolute value) translation, frequencies are doubled in velocity and acceleration frequency spectrum, which means that the real predominant frequency of oscillation movement is only half the value of output DF.

According to the observation, the absolute value of velocity would decrease to the lowest value every time when oscillation comes to a turning point, which means that it is possible to reconstruct the original velocity spectrum if the spectrum of absolute velocity on the right side of the point is flipped upside down every time when a nadir of absolute velocity comes. With this true velocity spectrum, it is plausible to translate it into deviation spectrum via integral transform. This is a possible method of unwrapping. Unfortunately, during this study, formulas developed for this section only reconstruct the expected frequency spectrum of velocity but not the frequency spectrum of acceleration, which means though the ‘doubled’ frequencies turn out to be ‘halved’ as anticipated, the translation function has not fulfilled for all the requirements. To develop plausible transformation algorithm, further meticulous feature extraction of the ‘doubling’ and corresponding ‘halving’ are required.

3. DF: Peak Value or Bump Area

In the 2012 study [77] and this study, amplitude of predominant frequency (DFA) was used as an integrative indicator of severity. However, as stated in introduction chapter and patient data displayed in this report, rather than a sharp spike, the predominant frequencies usually have a bandwidth. This raises the debate of whether it should be amplitude of the peak or the area under the peak to represent the severity of tremor and how to get the value in the case of the second parameter.

The problems with calculating the area under the peak generally are edge definition and normalization methods. Regarding to the first issue, there are questions like where does the bump start, where does it end, is there a threshold and how to find it, should the shape of the bump be modified considering noise and how, what happen to the cases where this peak is asymmetric, and so on. The answers to those questions should take in account of both signal processing and interpretations in medical science because they have to be mathematically proven and make clinical sense to physicians. Considering the shape of curve, the first issue is the edge definition so that characteristic feature extraction of the bump could be conducted. Secondly, because the simulation model need to match the corresponding ‘bump’ to provide a reliable comparable value and that the shape of this ‘bump’ differs from patient to patient, generation of shape model should be developed for each patient recording.

4. Full Automation Availability

Two major tasks in automation processing include 1) choose rotation angle in spatial domain processing and 2) predominant frequency peak in frequency spectrum analysis.

The former task, with the help of radon information, needs further sophisticated algorithm to optimize the results. The latter is more depending on the nature of the patterns of the recording.

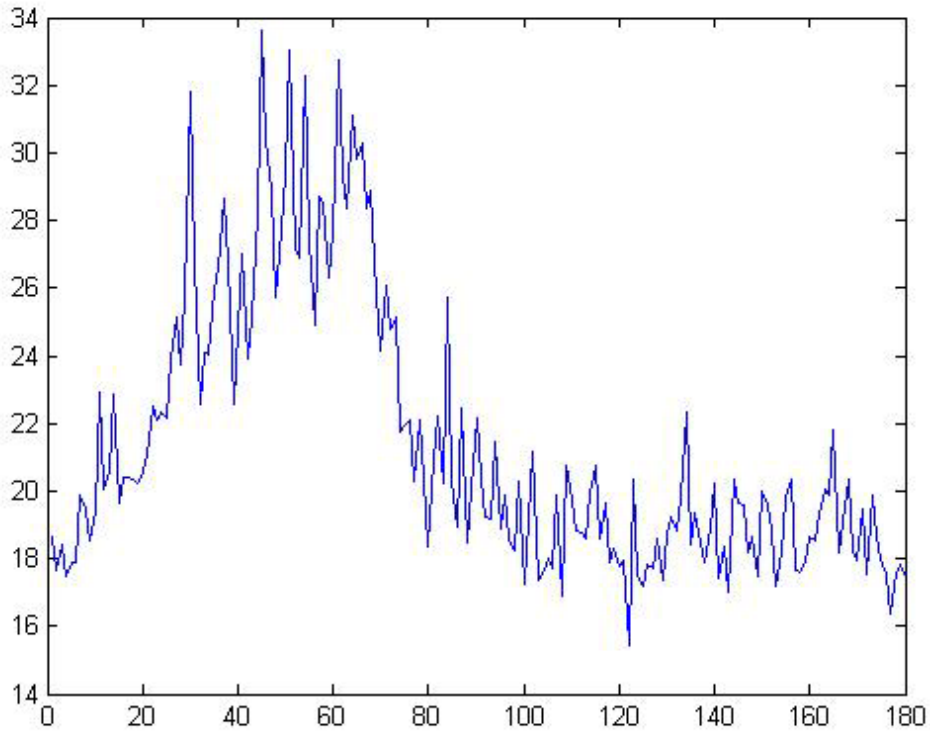

Figure V.5.1. Max(radon) distribution 1. In this figure, values on x axis indicate the angle of radon projections, values on y axis are the maximum value of each projection profile. The preferable rotation angle for the patient recording from which this figure is obtained is around 50 degree.

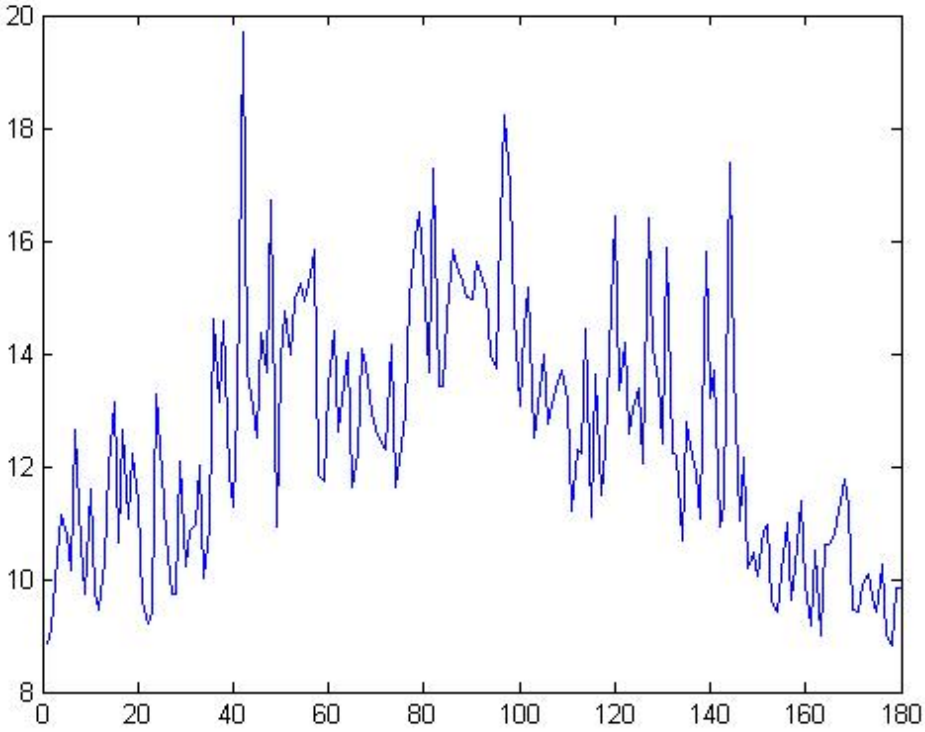

Figure V.5.2. Max(radon) distribution 2. The preferable rotation angle for the patient recording from which this figure is obtained is around 90 degree.

During the patient database process of this study, attempt of full automatic processing was made. The process was partially accomplished. The outcomes of the process contain issues relating to lability/instability owing to the ununiformity of the patient recordings. Generally, patient recordings in both databases could be divided into 2 categorizes: those with detectable/visible tremor and those that are basically smooth spirals aligned with model spiral with small smooth deviation. The second category does not show tremor oscillation. Though all patients who were asked to participate in database collecting are diagnosed ET patients, each individual patient does not necessarily have to have detectable tremor on the hand under recording. It is a fact that some patients have unilateral hand tremor instead of bilateral. In these case, those highly patterned frequency

peaks at 5Hz/10Hz/15Hz/20Hz/25Hz are noise signal due to sampling and spatial digitizing (generally these noise signals rise regularly, approximately every 5Hz, after low pass filtering only peaks below 25Hz are able to be shown in the results.)

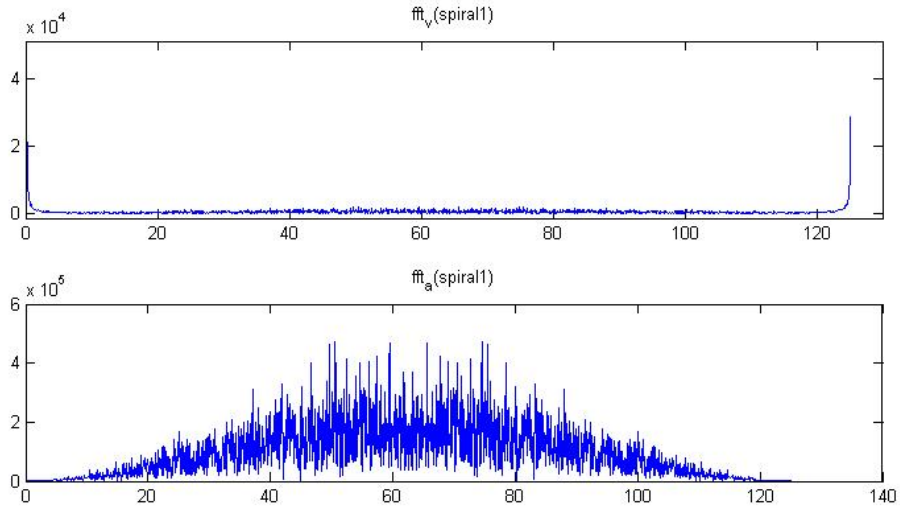

Figure V.5.3. Smooth Spiral1 frequency spectrum (noises in tremor frequency spectrum).

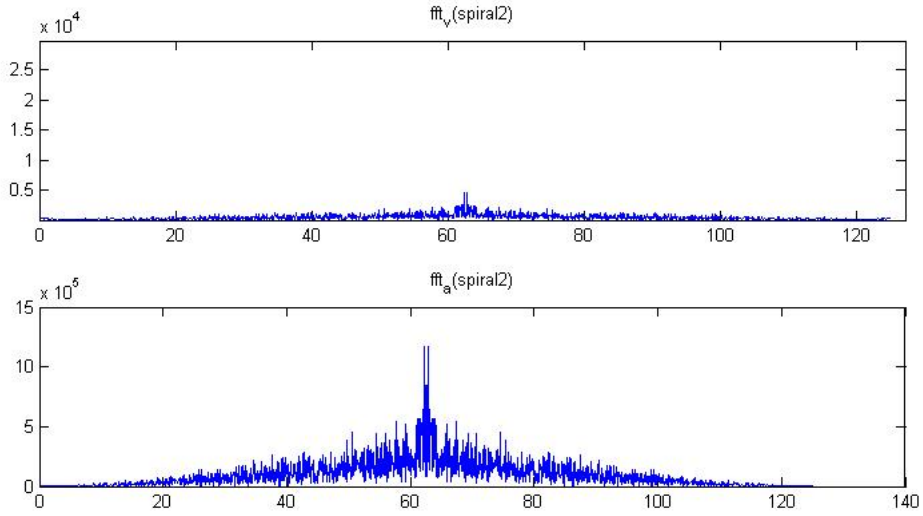

Figure V.5.4. Smooth Spiral2 frequency spectrum (noises in tremor frequency spectrum).

To deal with the non-tremor issue threshold were drew to determine whether there is tremor expressed in each recording so as to imply whether the supposedly followed processing and results are applicable. The larger issue with automation liability is with the recordings with unuiformed tremor symptom.

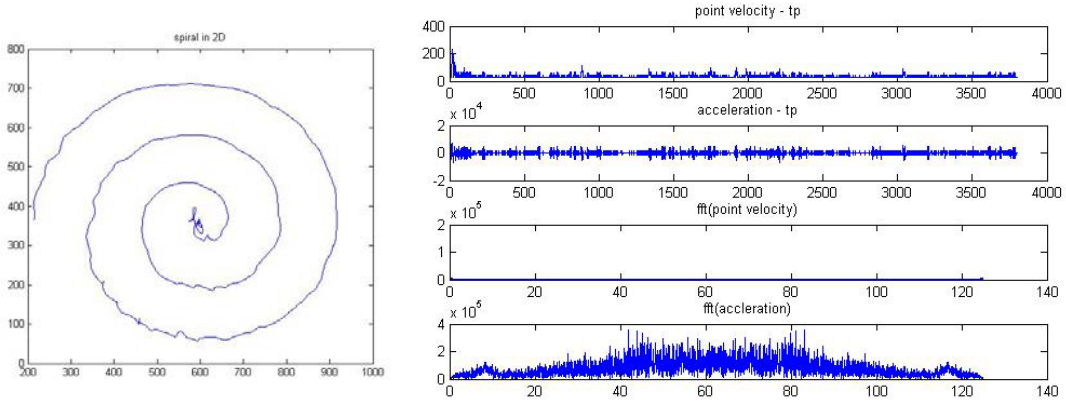

Figure V.5.5. Uniform distribution of low amplitude tremor oscillation, on the left is the final image of a patient recording, on the right is the frequency spectrum of this recording. It can be seen in the spectrum that tremor information is buried by noise (smooth spiral) signals.

In some patient recordings, oscillation only exist at some certain radian pocket, the drawing trace outside the pocket is basically a fine smooth spiral. In these cases, the amplitude of tremor information in frequency spectrum is so small that they are buried by the noise signals from the rest part of the recording (the smooth spiral part.) As demonstrated in Chapter IV, spatial domain analysis is conducted by extracting information from a defined window-view. Under automatic process, the location of this window is predetermined. As a result, they may or may not cover the part of the recording that contains oscillation information which would lead to the liability of outcome data. Besides ununiformity, a small portion of the patient recordings show more than one oscillation axes simultaneously or alternatively. For these cases, spirography

alone is not sufficient for diagnosis or monitoring. Further test with accelerometer could distinguish and isolate each individual oscillation movement.

WORKS CITED

1. Louis ED. Essential tremor. Lancet Neurol 2005;4:100–10.

2. Quinn NP, Schneider SA, Schwingenschuh P, Bathia KP. Tremor – Some controversial aspects. Mov Disord 2011;26:18–23.

3. Elble R, Deuschl G. Milestones in tremor research. Mov Disord 2011;26:1096–105.

4. Koller WC, Hubble JP, Busenbark KL. Essential tremor. In: Calne D. Neurodegenerative Diseases. Philadelphia: W.B. Saunders; 1994, pp. 717–42.

5. Deuschl G, Bain P, Brin M. Consensus statement of the movement disorder society on tremor. Mov Disord 1998;13:2–23.

6. Louis ED, Wendt KJ, Pullman SL, Ford B. Is essential tremor symmetric? Observational data from a community-based study of essential tremor. Arch Neurol 1998;55:1553–9.

7. Louis ED, Ferreira JJ. How common is the most common adult movement disorder? Update on the worldwide prevalence of essential tremor. Mov Disord 2010;25:534–41.

8. Deuschl G, Elble R. Essential tremor – Neurodegenerative or nondegenerative disease towards a working definition of ET. Mov Disord 2009;24:2033–41.

9. Rautakorpi I, Takala J, Marttila RJ, Sievers K, Rinne UK. Essential tremor in a Finnish population. Acta Neurol Scand 1982;66:58–67.

10. DoguO,SevimS,CamdevirenH,SasmazT,BugdayciR,AralM,etal.Prevalenceof essential tremor: door-to-door neurologic exams in Mersin Province, Turkey. Neurology 2003;61:1804–6.

11. Higgins JJ, Pho LT, Nee LE. A gene (ETM) for essential tremor maps to chromosome 2p22–p25. Mov Disord 1997;12:859–64.

12. Gulcher JR, Jonsson P, Kong A, Kristjansson K, Frigge ML, Karason A, et al. Mapping of a familial essential tremor gene, FET1, to chromosome 3q13. Nat Genet 1997;17:84–7.

13. Shatunov A, Sambuughin N, Jankovic J, Elble R, Lee HS, Singleton AB, et al. Genomewide scans in North American families reveal genetic linkage of essential tremor to a region on chromosome 6p23. Brain 2006;129:2318–31.

14. Deng H, Le W, Jankovic J. Genetics of essential tremor. Brain 2007;130:1456–64.

15. Tanner CM, Goldman SM, Lyons KE, Aston DA, Tetrud JW, Welsh MD, et al. Essential tremor in twins: an assessment of genetic vs environmental determinants of etiology. Neurology 2001;57:1389–91.

16. Louis ED. Etiology of essential tremor: should we be searching for environmental causes? Mov Disord 2001;16:822–9.

17. Dogu O, Louis ED, Tamer L, Unal O, Yilmaz A, Kaleagasi H. Elevated blood lead concentrations in essential tremor: a case-control study in Mersin, Turkey. Environ Health Perspect 2007;115:1564–8.

18. Louis ED. Environmental epidemiology of essential tremor. Neuroepidemiology 2008;31:139–49.

19. Louis ED, Jiang W, Pellegrino KM, Rios E, Factor-Litvak P, Henchcliffe C, et al. Elevated blood harmane (1-methyl-9h-pyrido[3,4-b]indole) concentrations in essential tremor. Neurotoxicology 2008;29:294–300.

20. Singer C, Sanchez-Ramos J, Weiner WJ. Gait abnormality in essential tremor. Mov Disord 1994;9:193–6.

21. Stolze H, Petersen G, Raethjen J, Wenzelburger R, Deuschl G. The gait disorder of advanced essential tremor. Brain 2001;124:2278–86.

22. Hubble JP, Busenbark KL, Pahwa R, Lyons K, Koller WC. Clinical expression of essential tremor: effects of gender and age. Mov Disord 1997;12:969–72.

23. Parisi SL, Heroux ME, Culham EG, Norman KE. Functional mobility and postural control in essential tremor. Arch Phys Med Rehabil 2006;87:1357–64.

24. Klebe S, Stolze H, Grensing K, Volkmann J, Wenzelburger R, Deuschl G. Influence of alcohol on gait in patients with essential tremor. Neurology 2005;65:96–101.

25. Deuschl G, Wenzelburger R, Loffler K, Raethjen J, Stolze H. Essential tremor and cerebellar dysfunction clinical and kinematic analysis of intention tremor. Brain 2000;123(Pt 8):1568–80.

26. Koster B, Deuschl G, Lauk M, Timmer J, Guschlbauer B, Lucking CH. Essential tremor and cerebellar dysfunction: abnormal ballistic movements. J Neurol Neurosurg Psychiatry 2002;73:400–5.

27. Leegwater-Kim J, Louis ED, Pullman SL, Floyd AG, Borden S, Moskowitz CB, et al. Intention tremor of the head in patients with essential tremor. Mov Disord 2006;21:2001–5.

28. Dupuis MJ, Delwaide PJ, Boucquey D, Gonsette RE. Homolateral disappearance of essential tremor after cerebellar stroke. Mov Disord 1989;4:183–7.

29. Schuurman PR, Bosch DA, Bossuyt PM, Bonsel GJ, van Someren EJ, de Bie RM, et al. A comparison of continuous thalamic stimulation and thalamotomy for suppression of severe tremor. N Engl J Med 2000;342:461–8.

30. Benabid AL, Pollak P, Seigneuret E, Hoffmann D, Gay E, Perret J. Chronic vim thalamic stimulation in Parkinson's disease, essential tremor and extra-pyramidal dyskinesias. Acta Neurochir Suppl 1993;58:39–44 (Wien).

31. Bucher SF, Seelos KC, Dodel RC, Reiser M, Oertel WH. Activation mapping in essential tremor with functional magnetic resonance imaging. Ann Neurol 1997;41:32–40.

32. Colebatch JG, Findley LJ, Frackowiak RS, Marsden CD, Brooks DJ. Preliminary report: activation of the cerebellum in essential tremor. Lancet 1990;336:1028–30.

33. Brooks DJ. Detection of preclinical Parkinson's disease with PET. Neurology 1991;41:24–7 discussion 28.

34. Brooks DJ, Playford ED, Ibanez V, Sawle GV, Thompson PD, Findley LJ, et al. Isolated tremor and disruption of the nigrostriatal dopaminergic system: an 18f- dopa PET study. Neurology 1992;42:1554–60.

35. Hallett M, Dubinsky RM. Glucose metabolism in the brain of patients with essential tremor. J Neurol Sci 1993;114:45–8.

36. Jenkins IH, Bain PG, Colebatch JG, Thompson PD, Findley LJ, Frackowiak RS, et al. A positron emission tomography study of essential tremor: evidence for overac- tivity of cerebellar connections. Ann Neurol 1993;34:82–90.

37. Wills AJ, Jenkins IH, Thompson PD, Findley LJ, Brooks DJ. Red nuclear and cerebellar but no olivary activation associated with essential tremor: a positron emission tomographic study. Ann Neurol 1994;36:636–42.

38. Wills AJ, Jenkins IH, Thompson PD, Findley LJ, Brooks DJ. A positron emission tomography study of cerebral activation associated with essential and writing tremor. Arch Neurol 1995;52:299–305.

39. Boecker H, Wills AJ, Ceballos-Baumann A, Samuel M, Thompson PD, Findley LJ, et al. The effect of ethanol on alcohol-responsive essential tremor: a positron emission tomography study. Ann Neurol 1996;39:650–8.

40. Louis ED, Shungu DC, Chan S, Mao X, Jurewicz EC, Watner D. Metabolic abnormality in the cerebellum in patients with essential tremor: a proton magnetic resonance spectroscopic imaging study. Neurosci Lett 2002;333:17–20.

41. Pagan FL, Butman JA, Dambrosia JM, Hallett M. Evaluation of essential tremor with multi-voxel magnetic resonance spectroscopy. Neurology 2003;60:1344–7.

42. Jasinska-Myga B, Wider C. Genetics of essential tremor. Parkinsonism and Related Disorders 18S1 (2012) S138–S139

43. Louis ED, Ford B, Barnes LF. Clinical subtypes of essential tremor. Arch Neurol 2000;57:1194–8.

44. Louis ED. Essential tremor as a neuropsychiatric disorder. Journal of the Neurological Sciences 2010:289:144–148

45. Rajput AH, Rozdilsky B, Ang L, Rajput A. Significance of parkinsonian manifestations in essential tremor. Can J Neurol Sci 1993;20:114–7.

46. Koller WC, Rubino FA. Combined resting-postural tremors. Arch Neurol 1985:42:683–4.

47. Cohen O, Pullman S, Jurewicz E, Watner D, Louis ED. Rest tremor in patients with essential tremor: prevalence, clinical correlates, and electrophysiologic char- acteristics. Arch Neurol 2003;60:405–10.

48. Brennan KC, Jurewicz EC, Ford B, Pullman SL, Louis ED. Is essential tremor predominantly a kinetic or a postural tremor? A clinical and electrophysiological study. Mov Disord 2002;17:313–6.

49. Louis ED, Rios E, Applegate LM, Hernandez NC, Andrews HF. Jaw tremor: prevalence and clinical correlates in three essential tremor case samples. Mov Disord 2006;21:1872–8.

50. Louis ED, Ford B, Frucht S. Factors associated with increased risk of head tremor in essential tremor: a community-based study in northern Manhattan. Mov Disord 2003;18:432–6.

51. Louis ED. Essential tremor. Lancet Neurol 2005;4:100–10.

52. Leegwater-Kim J, Louis ED, Pullman SL, Floyd AG, Borden S, Moskowitz CB, Honig LS. Intentional tremor of the head in patients with essential tremor. Mov Disord 2006;21:2001–5.

53. Louis ED, Dogu O. Isolated head tremor: Part of the clinical spectrum of essential tremor? Data from population-based and clinic-based case samples. Mov Disord 2009;24:2281–5.
54. Louis ED, Rios E, Applegate LM, Hernandez NC, Andrews HF. Jaw tremor: Prevalence and clinical correlates in three essential tremor case samples. Mov Disord 2006;21:1872–8.

55. Dooneief G, Mirabello E, Bell K, Marder K, Stern Y, Mayeux R. An estimate of theincidence of depression in idiopathic Parkinson's disease. Arch Neurol 1992;49:305–7.

56. Stern Y, Marder K, Tang MX, Mayeux R. Antecedent clinical features associated with dementia in Parkinson's disease. Neurology 1993;43:1690–2.

57. Mayeux R, Stern Y, Rosenstein R, Marder K, Hauser A, Cote L, et al. An estimate of the prevalence of dementia in idiopathic Parkinson's disease. Arch Neurol1988;45:260–2.

58. Marder K, Mayeux R. The epidemiology of dementia in patients with Parkinson's disease. Adv Exp Med Biol 1991;295:439–45.

59. Gasparini M, Bonifati V, Fabrizio E, Fabbrini G, Brusa L, Lenzi GL, et al. Frontal lobe dysfunction in essential tremor: a preliminary study. J Neurol 2001;248:399–402.

60. Lombardi WJ, Woolston DJ, Roberts JW, Gross RE. Cognitive deficits in patients with essential tremor. Neurology 2001;57:785–90.

61. Duane DD, Vermilion KJ. Cognitive deficits in patients with essential tremor. Neurology 2002;58:1706 author reply 1706.

62. Lacritz LH, Dewey Jr R, Giller C, Cullum CM. Cognitive functioning in individuals with “benign” essential tremor. J Int Neuropsychol Soc 2002;8:125–9.

63. Troster AI, Woods SP, Fields JA, Lyons KE, Pahwa R, Higginson CI, et al. Neuropsychological deficits in essential tremor: an expression of cerebello-thalamo-cortical pathophysiology? Eur J Neurol 2002;9:143–51.

64. Benito-Leon J, Louis ED, Bermejo-Pareja F. Population-based case-control study of cognitive function in essential tremor. Neurology 2006;66:69–74.

65. Sahin HA, Terzi M, Ucak S, Yapici O, Basoglu T, Onar M. Frontal functions in young patients with essential tremor: a case comparison study. J Neuropsychiatry Clin Neurosci 2006;18:64–72.

66. Benito-Leon J, Louis ED, Bermejo-Pareja F. Elderly-onset essential tremor is associated with dementia. Neurology 2006;66:1500–5.

67. S.T. Thawani SN, E.D. Louis, Association between essential tremor and dementia: population-based study in New York, in press.

68. Chatterjee A, Jurewicz EC, Applegate LM, Louis ED. Personality in essential tremor: further evidence of non-motor manifestations of the disease. J Neurol Neurosurg Psychiatry 2004;75:958–61.

69. Tan EK, Fook-Chong S, Lum SY, Gabriel C, Koh KK, Prakash KM, et al. Non-motor manifestations in essential tremor: use of a validated instrument to evaluate a wide spectrum of symptoms. Parkinsonism Relat Disord 2005;11:375–80.

70. Miller KM, Okun MS, Fernandez HF, Jacobson CEt, Rodriguez RL, Bowers D. Depression symptoms in movement disorders: comparing Parkinson's disease, dystonia, and essential tremor. Mov Disord 2007;22:666–72.

71. Louis ED, Benito-Leon J, Bermejo-Pareja F. Self-reported depression and anti-depressant medication use in essential tremor: cross-sectional and prospective analyses in a population-based study. Eur J Neurol 2007;14:1138–46.

72. Dogu O, Louis ED, Sevim S, Kaleagasi H, Aral M. Clinical characteristics of essential tremor in Mersin, Turkey—a population-based door-to-door study. J Neurol 2005;252:570–4.

73. Louis ED, Barnes L, Albert SM, Cote L, Schneier FR, Pullman SL, et al. Correlates of functional disability in essential tremor. Mov Disord 2001;16:914–20.

74. Schneier FR, Barnes LF, Albert SM, Louis ED. Characteristics of social phobia among persons with essential tremor. J Clin Psychiatry 2001;62:367–72.

75. Louis ED. Behavioral symptoms associated with essential tremor. Adv Neurol 2005;96:284–90.

76. Findley LJ. Expanding clinical dimensions of essential tremor. J Neurol Neurosurg Psychiatry 2004;75:948–9

77. Sargolzari S. Impact of accelerometry and spirography data analysis of essential tremor on BOLD-fMRI data interpretation. University of Miami Scholarly Repository 2012; Open Access Thesis. Paper 309

No	FILENAME	L/R	DF	UDFAV	NDFAV	UDFAA	NDFAA	Amp_min	Amp_max	tp
1	'P01_baseline_R-1'	'r'	'N/A'	'N/A'	'N/A'	'N/A'	'N/A'	'N/A'	'N/A'	3891
2	'P01_baseline_R-2'	'r'	'N/A'	'N/A'	'N/A'	'N/A'	'N/A'	'N/A'	'N/A'	3898
3	'P01_inderal_R-1'	'r'	'N/A'	'N/A'	'N/A'	'N/A'	'N/A'	'N/A'	'N/A'	2895
4	'P01_inderal_R-2'	'r'	'N/A'	'N/A'	'N/A'	'N/A'	'N/A'	'N/A'	'N/A'	2986
5	'P02_baseline_R-1'	'r'	10.5388	4541.329	7680.172	294336.8	497774.5	2.125	3.375	1364
6	'P02_baseline_R-2'	'r'	11.0833	3403.942	4156.848	231747.7	283007.2	0.875	2.25	1500
7	'P02_etoh_R-1'	'r'	4.65530	8022.5	18719.83	228994.9	534340.4	'N/A'	'N/A'	1262
8	'P02_etoh_R-2'	'r'	5.10734	6842.891	12312.42	215468.6	387692.8	'N/A'	'N/A'	1444
9	'P02_inderal_R-1'	'r'	5.53678	13319.14	25289.33	452268.7	858731.6	0.625	3.25	1332
10	'P02_inderal_R-2'	'r'	5.56983	13134.62	31929.1	448892.1	1091218	0.75	2.5625	1167
11	'P03_baseline_R-1'	'r'	12.2810	5812.204	3504.297	438959.6	264657.7	0.25	2.125	3369
12	'P03_baseline_R-2'	'r'	13.562	4057.731	2441.678	337897.6	203324.7	0.125	1.625	3235
13	'P04_baseline_R-1'	'r'	10.198	16038.97	11549.05	1009346	726791.5	0.25	9.5	3225
14	'P04_baseline_R-2'	'r'	9.53698	13321.25	8238.512	794693.1	491477.1	0.75	4.125	3434
15	'P05_baseline_R-1'	'r'	'N/A'	'N/A'	'N/A'	'N/A'	'N/A'	'N/A'	'N/A'	2231
16	'P05_baseline_R-2'	'r'	'N/A'	'N/A'	'N/A'	'N/A'	'N/A'	'N/A'	'N/A'	2390
17	'P05_inderal_R-1'	'r'	5.83852	4900.38	4815.66	177899.1	174823.5	'N/A'	'N/A'	2248
18	'P05_inderal_R-2'	'r'	5.88642	5983.341	5028.842	217670.2	182946.1	'N/A'	'N/A'	2166
19	'P06_baseline_R-1'	'r'	5.65403	4691.28	3250.721	163009.3	112953.8	'N/A'	'N/A'	2454
20	'P06_baseline_R-2'	'r'	6.11463	5043.409	3608.443	191590.5	137078.6	0	1.625	2678
21	'P06_inderal_R-1'	'r'	6.22119	7733.478	6871.364	298346.5	265087.3	0.125	1.5	2170
22	'P06_inderal_R-2'	'r'	7.25362	4235.49	4049.651	188084.7	179832.2	'N/A'	'N/A'	1999
23	'P07_baseline_R-1'	'r'	'N/A'	'N/A'	'N/A'	'N/A'	'N/A'	'N/A'	'N/A'	2118

No.	FILENAME	L/R	DF	UDFAV	NDFAV	UDFAA	NDFAA	Amp_min	Amp_max	tp
24	'P07_baseline_R-2'	'r'	9.504052	82374.58	52899.13	4845253	3111514	0.875	10.625	2591
25	'P08_baseline_R-1'	'r'	5.575117	9871.675	20923.25	338865.7	718234	'N/A'	'N/A'	1278
26	'P08_baseline_R-2'	'r'	5.455112	9892.156	13705.36	333545.1	462119.1	0.75	1.375	1604
27	'P08_inderal_R-1'	'r'	5.387144	8691.846	14324.37	289278.1	476737.1	'N/A'	'N/A'	1369
28	'P08_inderal_R-2'	'r'	5.338371	9297.157	13091.87	302974.2	426635.9	'N/A'	'N/A'	1522
29	'P09_baseline_R-1'	'r'	7.677023	5792.718	3748.772	276068.8	178658.6	'N/A'	'N/A'	2768
30	'P09_baseline_R-2'	'r'	7.146914	6272.959	5621.938	278071.9	249213	'N/A'	'N/A'	2641
31	'P09_inderal_R-1'	'r'	'N/A'	'N/A'	'N/A'	'N/A'	'N/A'	'N/A'	'N/A'	2770
32	'P09_inderal_R-2'	'r'	7.487359	2967.993	2659.269	139026.4	124565.1	'N/A'	'N/A'	2571
33	'P10_baseline_R-1'	'r'	'N/A'	'N/A'	'N/A'	'N/A'	'N/A'	'N/A'	'N/A'	1444
34	'P10_baseline_R-2'	'r'	'N/A'	'N/A'	'N/A'	'N/A'	'N/A'	'N/A'	'N/A'	1005
35	'P11_baseline_R-1'	'r'	'N/A'	'N/A'	'N/A'	'N/A'	'N/A'	'N/A'	'N/A'	2906
36	'P11_baseline_R-2'	'r'	'N/A'	'N/A'	'N/A'	'N/A'	'N/A'	'N/A'	'N/A'	2771
37	'P11_etoh_R-1'	'r'	'N/A'	'N/A'	'N/A'	'N/A'	'N/A'	'N/A'	'N/A'	3278
38	'P11_etoh_R-2'	'r'	'N/A'	'N/A'	'N/A'	'N/A'	'N/A'	'N/A'	'N/A'	3219
39	'P11_inderal_R-1'	'r'	'N/A'	'N/A'	'N/A'	'N/A'	'N/A'	'N/A'	'N/A'	2125
40	'P11_inderal_R-2'	'r'	'N/A'	'N/A'	'N/A'	'N/A'	'N/A'	'N/A'	'N/A'	2655
41	'P12_baseline_R-1'	'r'	13.13886	33666.28	12409.92	2737550	1009104	1.625	9.875	5185
42	'P12_baseline_R-2'	'r'	13.29558	30060.85	16642.01	2447700	1355073	1	4	3488
43	'P13_baseline_R-1'	'r'	'N/A'	'N/A'	'N/A'	'N/A'	'N/A'	'N/A'	'N/A'	3491
44	'P13_baseline_R-2'	'r'	8.519793	14455.18	7964.95	763564.8	420732	'N/A'	'N/A'	2905
45	'P13_etoh_R-1'	'r'	'N/A'	'N/A'	'N/A'	'N/A'	'N/A'	'N/A'	'N/A'	3804
46	'P13_etoh_R-2'	'r'	'N/A'	'N/A'	'N/A'	'N/A'	'N/A'	'N/A'	'N/A'	3400

No.	FILENAME	L/R	DF	UDFAV	NDFAV	UDFAA	NDFAA	Amp_min	Amp_max	tp
47	‘P13_inderal_R-1’	‘r’	[]	[]	[]	[]	[]	[]	[]	[]
48	'P13_inderal_R-2'	'r'	'N/A'	'N/A'	'N/A'	'N/A'	'N/A'	'N/A'	'N/A'	3656
49	'P14_baseline_R-1'	'r'	'N/A'	'N/A'	'N/A'	'N/A'	'N/A'	'N/A'	'N/A'	1755
50	'P14_baseline_R-2'	'r'	'N/A'	'N/A'	'N/A'	'N/A'	'N/A'	'N/A'	'N/A'	1352
51	'P14_inderal_R-1'	'r'	'N/A'	'N/A'	'N/A'	'N/A'	'N/A'	'N/A'	'N/A'	1163
52	'P14_inderal_R-2'	'r'	'N/A'	'N/A'	'N/A'	'N/A'	'N/A'	'N/A'	'N/A'	2366
53	'P15_baseline_R-1'	'r'	5.650022	4784.528	3813.147	167109.4	133182	'N/A'	'N/A'	2323
54	'P15_baseline_R-2'	'r'	'N/A'	'N/A'	'N/A'	'N/A'	'N/A'	'N/A'	'N/A'	3867
55	'P15_etoh_R-1'	'r'	'N/A'	'N/A'	'N/A'	'N/A'	'N/A'	'N/A'	'N/A'	3827
56	'P15_inderal_R-1'	'r'	'N/A'	'N/A'	'N/A'	'N/A'	'N/A'	'N/A'	'N/A'	3106
57	'P15_inderal_R-2'	'r'	'N/A'	'N/A'	'N/A'	'N/A'	'N/A'	'N/A'	'N/A'	3239
58	'P16_baseline_R-1'	'r'	'N/A'	'N/A'	'N/A'	'N/A'	'N/A'	'N/A'	'N/A'	1859
59	'P16_baseline_R-2'	'r'	'N/A'	'N/A'	'N/A'	'N/A'	'N/A'	'N/A'	'N/A'	1672
60	'P16_etoh_R-1'	'r'	'N/A'	'N/A'	'N/A'	'N/A'	'N/A'	'N/A'	'N/A'	1338
61	'P16_etoh_R-2'	'r'	'N/A'	'N/A'	'N/A'	'N/A'	'N/A'	'N/A'	'N/A'	1275
62	'P16_inderal_R-1'	'r'	'N/A'	'N/A'	'N/A'	'N/A'	'N/A'	'N/A'	'N/A'	2402
63	'P16_inderal_R-2'	'r'	'N/A'	'N/A'	'N/A'	'N/A'	'N/A'	'N/A'	'N/A'	1890
64	'P17_baseline_R-1'	'r'	'N/A'	'N/A'	'N/A'	'N/A'	'N/A'	'N/A'	'N/A'	3532
65	'P17_baseline_R-2'	'r'	'N/A'	'N/A'	'N/A'	'N/A'	'N/A'	'N/A'	'N/A'	3502
66	'P17_etoh_R-1'	'r'	'N/A'	'N/A'	'N/A'	'N/A'	'N/A'	'N/A'	'N/A'	1631
67	'P17_etoh_R-2'	'r'	'N/A'	'N/A'	'N/A'	'N/A'	'N/A'	'N/A'	'N/A'	1311